

Cell Cycle of *Emiliana huxleyi* and its effects on host:virus interactions

Rebecca Louise Jefferson

Thesis submitted to the University of Plymouth
in partial fulfilment of the requirements for the degree of

MRes Marine Biology

**University of Plymouth
Faculty of Science**

in collaboration with

**Marine Biological Association, Plymouth, UK
Plymouth Marine Laboratory, Plymouth, UK**

September 2004

90 0719498 3



REFERENCE USE ONLY

University of Plymouth
Library

Item No. 9007194983

Shelfmark
THESIS 578.77 JEF

Copyright Statement

This copy of the thesis has been supplied on condition that anyone who consults it is understood to recognise that its copyright rests with the author and that no quotation from the thesis and no information derived from it may be published without the author's prior written consent.

Abstract

Emiliana huxleyi is an ecologically important marine phytoplankton and it is regularly forms large blooms. Viruses are an important agent of mortality in blooms, however, little is known about the host:virus interactions in this system. This project investigated how infection at different stages of the host cell cycle influenced: virus adsorption, infection and production and host lysis and cell cycle.

Cultures were infected during the G1, S or G2 + M phase and monitored for 2 hours for adsorption and infection or monitored for 48 hours for virus production, host lysis and host cell cycle. A three fold increase in infection during the G2 + M phase was recorded, however there was no significant difference in virus adsorption or virus production between phases. Cultures infected in the G2 + M phase lysed faster than cultures infected G1 or S phase and there was a three fold increase in infection success if infected during the G2 + M phase. This may be due to changes in the host at the point of cell division. All cultures showed a deviation from the normal cell cycle activity after 24 hours of infection and remained in a stable, compromised state after this point.

Virus production was independent of infection phase, this result may have been an artefact of the virulent nature of the system as the infected hosts began to lyse 4 hours after infection enabling a constant supply of viruses and repeated infections outside the initial phase of infection.

The ecological significance of these findings is believed to maintain a variation in virus production and host loss which allows both components of the systems to perpetuate.

Contents

1. Introduction	1
1.1. Overview and Aims	1
1.2. Oceanic Ecosystems and Laboratory-based Experiments	3
1.3. <i>Emiliana huxleyi</i>	4
1.3.1. Coccoliths, structure and production	5
1.3.2. <i>Emiliana huxleyi</i> blooms	5
1.3.3. <i>Emiliana huxleyi</i> and the carbon cycle	6
1.3.4. <i>Emiliana huxleyi</i> , Dimethylsulphide and Global Climate	7
1.4. Cell Cycle and Life Cycle Phase in Marine Phytoplankton	8
1.5. Viruses	12
1.5.1. Viruses in Phytoplankton	12
1.5.2. Viruses in <i>Emiliana huxleyi</i> blooms	14
1.6. Virus Effects on Hosts	16
1.7. Overall Summary	16
2. Materials and Methods	17
2.1. Materials	17
2.1.1. <i>f/2</i>	17
2.1.2. Buffers and Solutions	18
2.1.3. Microalgae Cultures	18
2.1.4. Viruses	19
2.2. Methods	19
2.2.1. Analytical Flow Cytometry	19
2.2.1.1. Virus Enumeration	19
2.2.1.2. Host Enumeration	20
2.2.1.3. Cell Cycle Analysis	20
2.2.2. Plaque Assays	23
2.2.2.1. Preparations	23
2.2.2.2. Samples	23
2.2.3. Infection Experiments	24
2.2.3.1. Virus Samples	24
2.2.3.2. Cell Cycle Samples	25
2.2.3.3. Host Numbers	25

2.2.4. Adsorption Assay	25
2.2.5. Cell Cycle Tests	25
3. Cell Cycle Tests and Culture Ploidy Levels	27
3.1. Introduction	27
3.2. Results	28
3.3. Discussion	33
4. Results	35
4.1. Introduction	35
4.2. Infection Experiments	36
4.2.1. Cell cycle	36
4.2.1.1. Cell Cycle at Infection Points	36
4.2.1.2. Cell Cycle During Infection	36
4.2.2. Host Numbers	38
4.2.3. Virus Numbers	38
4.3. Adsorption Experiments	39
5. Additional observations during sample analysis	54
5.1. Live Host	54
5.2. Virus Population	55
6. Discussion	59
6.1. Infection Experiment One	59
6.2. Infection Experiment Two	60
6.3. Cell Cycle	62
6.3.1. Cell Cycle Tests	63
6.4. Adsorption and Infection	63
6.5. Virus Release	65
6.5.1. Confounding Effect	67
7. Conclusions	69
8. Suggestions for Further Work	72
9. References	73

List of Tables

Table 2.1 Components required for <i>f/2</i> media	17
Table 2.2 Components required for <i>f/2</i> trace metal solution	17
Table 2.3 Components required for <i>f/2</i> vitamin solution	18
Table 2.4 Buffers and solutions	18
Table 4.1 Cell Cycle Changes	37
Table 4.2 Time of culture collapse	38

List of Figures

Figure 1.1 <i>Emiliana huxleyi</i>	2
Figure 1.2 <i>Emiliana huxleyi</i> bloom	3
Figure 1.3 Cell cycle and light:dark cycle of <i>Emiliana huxleyi</i> cultures	9
Figure 1.4 Typical histograms during cell cycle phases	11
Figure 2.1 Typical virus AFC plot	22
Figure 2.2 Typical <i>Emiliana huxleyi</i> AFC plot	22
Figure 2.3 Typical cell cycle analysis plots	22
Figure 3.1 Cell cycle images from initial cell cycle test	30
Figure 3.2 Cell cycle images from second cell cycle test	31
Figure 3.3 Scatter plot showing increasing DNA within populations	32
Figure 4.1 Experimental design of infection experiments	40
Figure 4.2 Cell cycle histograms from infection experiments	42
Figure 4.3 Cell cycle scatter plots from infection experiments	45
Figure 4.4 Host numbers from infection experiments	47
Figure 4.5 Virus numbers from infection experiments	49
Figure 4.6 Plaque Assay results	51
Figure 4.7 Virus numbers during adsorption	52
Figure 5.1 <i>Emiliana huxleyi</i> populations during the infection experiments	57
Figure 5.2 Virus populations during the infection experiments	57
Figure 5.3 Changes in virus group location	58

Acknowledgements

I would like to thank Willie Wilson for his unfailing support and enthusiasm throughout my project and for teaching me marine microbiology.

Thank you Dr Declan Schroeder, Dr Vic Goddard and Dr Mike Allen for answering an endless stream of questions and always smiling; to Matt Hall for help in the lab, especially for the all night sampling session, to Jayme Lohr for keeping my sanity in check and to Andrea Baker, Joaquin Martinez-Martinez and everyone else in the research teams who have made this project an enjoyable experience.

Thanks to my Mum and Dad for their never ending support in everything I choose to do.

1. Introduction

1.1. Overview and Aims

There are many global environmental issues facing the world today. When considering issues of this magnitude, it is often easy to overlook the intricate workings of individual species in favour of a macro-ecology approach. This can be dangerous as the size of a species can belie the influences it is having on the planet.

One such species is *Emiliania huxleyi*. As a member of the coccolithophores (Family: *Haptophytae*), it is a unicellular phytoplankton, distinguished by the calcified coccolith plates which surround the cell to form a coccosphere (fig. 1.1). *E. huxleyi* is a cosmopolitan species and forms large blooms in both coastal and oceanic waters (fig. 1.2). Under bloom conditions, the great abundance of *E. huxleyi* leads to far reaching effects on biological, geological and chemical cycles. The effects of blooms can have both small and large scale impacts ranging from local ecosystem dynamics to global climate and the global carbon cycle.

Within the microbial ecosystems of blooms, viruses are known to be prevalent. In recent years it has been found that viruses are an important agent of mortality in *E. huxleyi* blooms (Wilson *et al.*, 2002a; Castberg *et al.*, 2001). Little is known about the host:virus interactions in this system. As the effects of blooms and their collapse have such far reaching impacts, it is important to understand to a greater extent the relationship between *E. huxleyi* and its viruses as this will hopefully, in turn lead to a better ability to understand the impacts of blooms.

The overall aim of this project is to investigate the host:virus relationship, in particular the infection process and virus production during different stages of the host cell cycle.

The aims of the project are:

To investigate whether virus production in *E. huxleyi* is cell cycle dependent:

- Does the success of infection vary depending upon which phase of the host cell cycle the infection takes place?
- Does one phase have a more efficient virus production than the others?
- Will the rate of virus adsorption vary between the different phases?
- Will the cell cycle change in any of the infected cultures? If changes occur, do these differ with the phase of infection?

The remainder of this chapter will provide a literature review of relevant areas, presenting the reader with an understanding of present knowledge in a number of areas: an introduction into *E. huxleyi* and its global impacts; an introduction to viruses in marine systems; and an overview of known host:virus interactions this, and other systems.

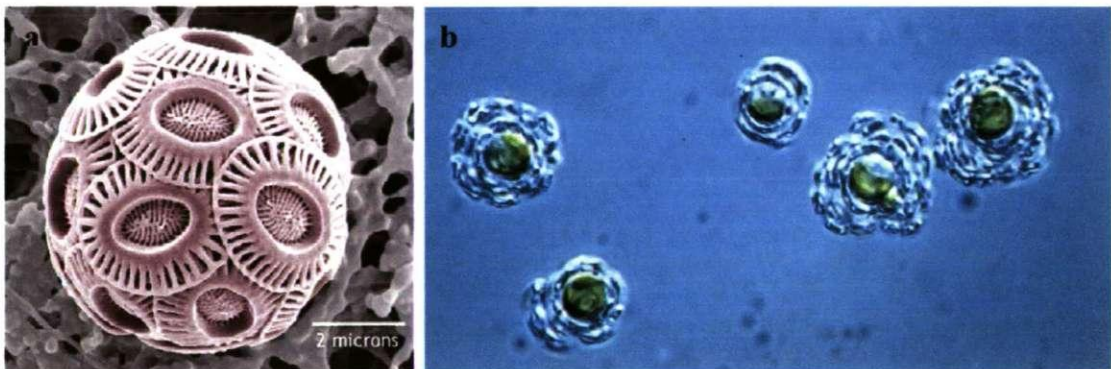


Figure 1.1 *E. huxleyi* seen with an electron microscope (a) and a light microscope (b). Individual coccoliths are clearly visible in a. The coccosphere is visible in both images as the coccoliths encase the cells.

Sources:

- a <http://earthguide.ucsd.edu/earthguide/imagelibrary/emilianiahuxleyi.html>
 b http://www.nhm.ac.uk/hosted_sites/ina/CODENET/galleries/DICimages/source/ehux.htm

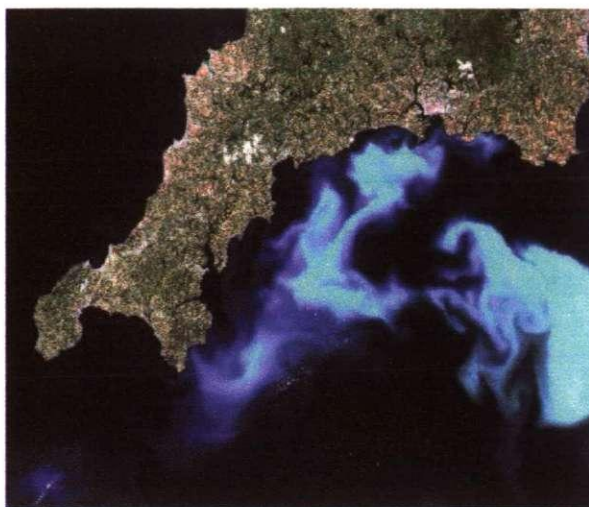


Figure 1.2 *Emiliana huxleyi* bloom off the south Devon and Cornwall coast, July 1999.

Source http://www.nhm.ac.uk/hosted_sites/ina/colourcoccos/source/z00-1_bloom_summer_99_.htm

1.2. Oceanic Ecosystems and Laboratory-Based Experiments

The overall aim of this project to study an open ocean system using laboratory techniques. Throughout the project, all conditions and equipment are monitored to ensure that the experiments are well controlled, not affected by changes in anything other than the desired variables, and are at the optimum natural conditions. However, there are aspects of this oceanic system which can never be duplicated in a laboratory based experiment, but that are important mechanisms within the system. There is a need to be aware of the differences between the conditions of these experiments and natural systems, especially as we use the conclusions drawn from laboratory experiments to better understand the workings of the natural systems.

All ecosystems have a cyclical nature and all components of the system are vulnerable to biotic and abiotic influences. Organisms have their specific inputs and outputs which in turn have roles in biogeochemical cycles. Biological systems are influenced by various disturbances, ranging from the normal diurnal and seasonal fluctuations in light and temperature through to daily climate variation and larger

disturbances such as storms or geological activity. All these factors and changes influence the system in the availability of key resources, and may have repercussions on the systems which we do not yet fully understand.

However, laboratory based cultures do not operate under normal conditions: they are not influenced by the usual wide variety of other organisms, the typical predator-prey and competition processes do not occur. Daily fluctuations are removed, e.g. change in day length, temperature, mixing of upper layers where *E. huxleyi* blooms are found which results in variances in light and nutrients, periodic disturbance events such as storms do not occur. We do not know how vital these characteristics of the system are and if they are an important part of the ecosystem which we are investigating – for example, allowing for a diversity which retains the essential interactions and yet prevents dominance by one species. This study does not focus on these interactions, but we still need to be aware of their function in our system.

Laboratory based experiments provide us with the best facilities to test hypotheses about organisms that we would be very difficult to test in their natural system. They allow us to perform well structured experiments from which we can gain an accurate representation of the behaviour of oceanic organisms and add to the understanding of these systems.

1.3. *Emiliana huxleyi*

E. huxleyi is a member of the coccolithophores. The most obvious feature of this unicellular phytoplankton is the calcium carbonate discs called coccoliths, which surround their cell to form a coccosphere (fig.1.1). Cells have a diameter of approximately 5µm (including the coccosphere). *E. huxleyi* is one of the most abundant of the coccolithophore species (Jordan, 2001) and is widely distributed: it is found in coastal and oceanic waters around the world, and is also unusually abundant in sub-

polar latitudes (Brand, 1994). Its poleward distribution is limited by the 0°C surface water isotherm (McIntyre *et al.*, 1970). Dominance of *E. huxleyi* varies slightly with season, and this is normally due to variation in the stratification of the water (Brand, 1994).

1.3.1. Coccoliths, Structure and Production

Coccoliths are the disc shaped plates which cover the cell of coccolithophores. They are composed of calcium carbonate and their structure, which differs between species, falls into two major groups: holococcoliths and heterococcoliths. These vary in production and structure: holococcoliths are constructed from large numbers of minute, but morphologically simple crystallites whereas heterococcoliths are constructed from radial arrays of complex crystal units (Young *et al.*, 1999). Holococcoliths are produced extracellularly on the cell membrane whereas the heterococcoliths are usually produced in a series of vesicles connected to the golgi body which begins with the formation of an organic base plate and are extruded to the coccosphere when fully formed. However, the heterococcoliths of *E. huxleyi* differ slightly as they do not possess a base plate and are produced in a specialised coccolith vesicle which is not associated with the golgi body. The function of coccoliths remains unknown, but it is suspected that it may be a combination of roles which are influenced by the environmental pressures (Young, 1994; Okado and Honjo, 1973).

1.3.2. *Emiliana huxleyi* Blooms

A number of phytoplankton species are able to form blooms: times when the correct conditions allow for rapid and large scale increases in a species' abundance. Some of these blooms can be dangerous to human health (Van Dolah *et al.*, 2001), such as *Pseudo-nitzschia australis* which causes Amnesic Shellfish Poisoning when infected

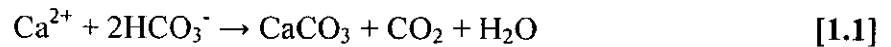
bivalves are eaten by humans. Blooms of *E. huxleyi* possess no threat to human health. *E. huxleyi* blooms are frequent annual events, especially in the temperate waters of the North Atlantic and can create spectacular occurrences, often visible from space due to the light refracting properties of the calcium within coccoliths (fig. 1.2). *E. huxleyi* blooms covered an average of 1.4×10^6 km² annually (Brown and Yoder, 1994) with individual blooms reaching an area over 100,000 km² with cell densities up to 10,000 ml⁻¹ (Tyrrell and Taylor, 1996). The greatest expanse of blooms is found in the Subarctic North Atlantic, with large blooms also being recorded in the North Pacific. Peak timings of blooms vary with latitude: subpolar blooms are more frequent in the summer to early autumn months whereas lower latitude blooms are more frequent during midwinter to early spring (Brown and Yoder, 1994).

Phytoplankton are the major primary producers in these ocean ecosystems. Under bloom conditions their inputs into the system increase considerably, upon collapse of the bloom, the quantity of dissolved organic matter released into the system is increasing and can have consequences on other components of the system. It is these conditions which allow such a small organism to be a major contributor to global scale cycles such as climate and the carbon cycle.

1.3.3. *Emiliana huxleyi* and the Carbon Cycle

Coccolith formation requires a large supply of calcium which is acquired from the surrounding seawater through calcification (formula 1.1). Together with the foraminifers, this process makes coccolithophores one of the major producers of biogenic calcite in the oceans (together with the foraminifers) (Riebesell *et al.*, 2000). Calcification in phytoplankton is a major component of the carbon cycle because the demand for calcium facilitates the uptake of carbon dioxide from the atmosphere. This process neutralises carbon dioxide and could act as a negative feedback on mechanism

carbon dioxide (Takahashi, 2004). This is important as oceans are a major sink for anthropogenic carbon dioxide (Sabine *et al.*, 2004).



Coccoliths can be lost from the coccosphere during the life of the cell (Klaveness and Paasche, 1979) but the major loss of coccoliths occurs when cells die. In bloom conditions, it is mainly coccoliths in the water column which are responsible for the satellite images of blooms as they refract light (fig. 1.2). The fate of detached coccoliths follows two possible paths: 45 – 65 % will be dissolved as pressure and acidity increases with depth (Feely *et al.*, 2004), enabling calcium carbonate stored in the coccoliths to precipitate out and be recycled. The remaining 35 – 55 % will settle out of suspension forming calcareous deposits (such deposits provide the primary stage in the geological formation of limestone and chalk lithology. The White Cliffs of Dover on the south coast of England are an example of previous large scale calcareous deposits.). These pathways complete the cycling of both the carbon and the calcium, either to a long term store in the sediments or as a short term use in the CaCO₃ cycle.

1.3.4. *Emiliana huxleyi*, Dimethylsulphide and Global Climate

A few phytoplankton are known to release dimethylsulfoniopropionate (DMSP); *E. huxleyi* is known to be a significant source of DMSP (Turner *et al.*, 1988; Malin *et al.*, 1993; Matrai & Keller, 1993). As DMSP breaks down, it forms dimethylsulfide (DMS), a gas which readily oxidises from a volatile sulphur compound in seawater to form sulphur dioxide and sulphuric acid. These gases provide a major source of natural acid rain. DMS may also have implications for global climate as it is thought to play an important role in climate regulation (Malin *et al.*, 1992). This is due to its ability to

form aerosols which have cloud condensation nuclei properties and are thought to be involved in a feedback loop whereby phytoplankton have some control over the amount of radiation reaching the sea surface (Charlson *et al.*, 1987). DMSP is released as cells die, when cells die, under conditions where a high number of cells are dying (such as under bloom conditions), a greater amount of DMSP is released leading to increased cloud formation. This in turn can cause a change in sunlight levels, reducing the amount of radiation reaching the phytoplankton and may lead to reduced growth rates of phytoplankton, thereby controlling the growth rate of the bloom.

These local changes have global effects due to the changes in radiation patterns and cloud albedo (Charlson *et al.*, 1987). In addition to this, DMS release accounts for over half of the nonanthropogenic gaseous sulphur atmospheric contributions (Bates *et al.*, 1992; Andreae 1990) making *E. huxleyi* an important organism in the sulphur cycle.

1.4. Cell Cycle and Life Cycle Phases in Marine Phytoplankton

Unicellular phytoplankton divides through asexual reproduction. As in all cells, a controlled process of cell and DNA growth and division enable this to occur: the cell cycle. In *E. huxleyi*, it takes 24 hours for one complete cell cycle which consists of a typical DNA division cycle with three main phases (fig. 1.3): the Gap 1 phase (G1) is the post mitosis phase; cells are growing in preparation for DNA synthesis which occurs during the S phase. After cell DNA has replicated, cells are either preparing for (G2: gap 2) or performing (M) mitosis, but have not completed cellular division (van Bleijswijk *et al.*, 1996). After division, cells are in the G1 phase and the cycle recurs.

Many components of phytoplankton biology are synchronised with their light:dark cycle, including the cell cycle (Chisholm, 1981). However, synchronicity does not signify control. The cell cycle is maintained by internal and external cues depending on the phase of the cycle. There is a species specific period in the cell cycle

where key environmental conditions can be responded to; if they are favourable to cell survival following division then the cell cycle will continue (Vaultot *et al.*, 1987). This occurs during the A – T segment (van Bleijswijk *et al.*, 1996). The cell cycle will arrest at point A if there is a particular environmental cue missing, e.g. diatoms are sensitive to temperature, light, nitrogen and silica levels, if any of these are insufficient then the cell will arrest. If all are satisfactory, the cell cycle continues to the transition point (T) where environmental factors are no longer inhibitory. After this point, the cell cycle is controlled by internal cues.

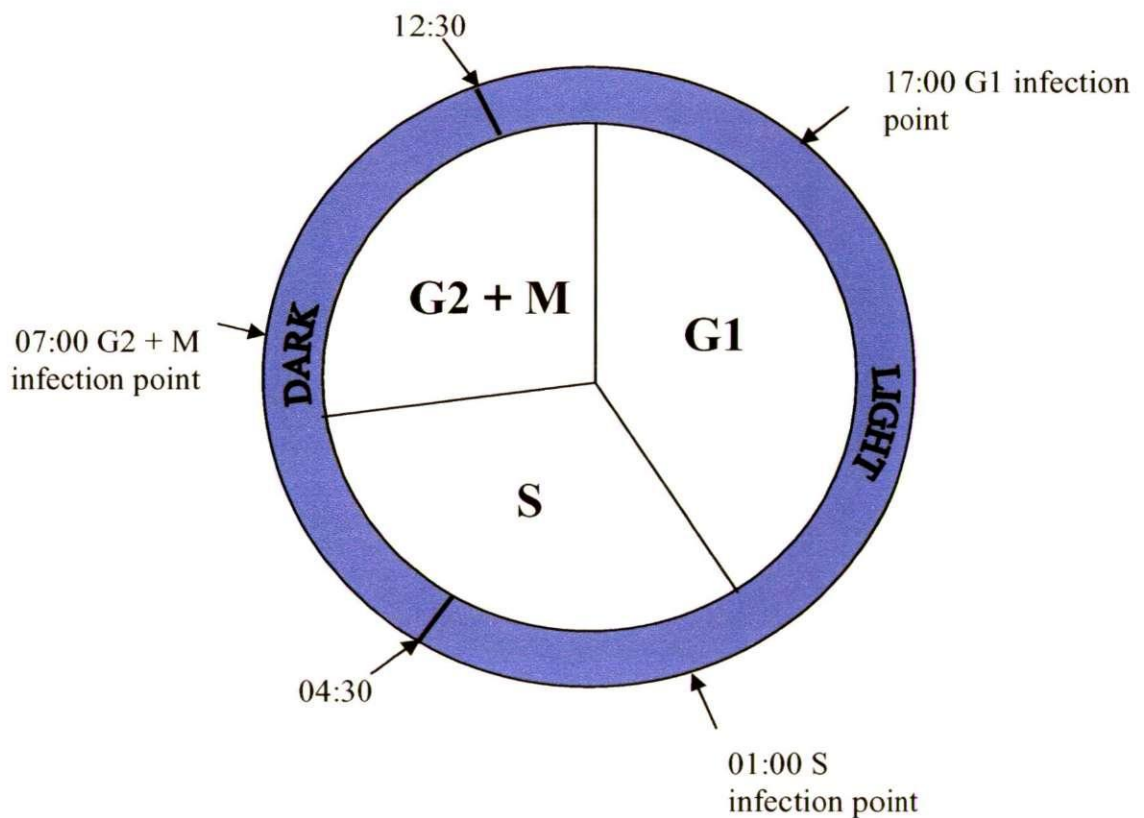


Figure 1.3 Diagrammatic representation of the cell cycle as it corresponds with the light:dark cycle

In *E. huxleyi*, internal cues appear to be very efficient at maintaining a specific cell cycle. Populations of different cell types and populations under different conditions

were found to vary considerably in the timing of the onset of DNA synthesis, but the maximum number of G2 + M cells was uniform between the populations (van Bleijswijk *et al.*, 1996). This suggests strong internal clock functions, occurring regardless of environmental and biological variations.

The division of DNA during the cell cycle is the key to its analysis. The amount of DNA in a cell can be measured using Analytical Flow Cytometry (section 2.2.1) and correlated with the cell cycle phase. If the amount of DNA in a cell is measured throughout a 24 cycle, it is possible to see where the DNA content of the cell doubles as it divides and then returns to the single copy value as the cell itself divides. Figure 1.4 shows the DNA frequency histograms and scatter plots predicted to be produced by an *E. huxleyi* population at each phase of the cell cycle using Analytical Flow Cytometry.

The life cycle of *E. huxleyi* is both complex and not well understood. It is known that a number of cell types exist: coccolith-bearing (C cells), non-motile and unlithed (naked or N cells) and motile, scale bearing (S cells). Each of these cell types can survive independently and reproduce vegetatively (Laguna *et al.*, 2001). S cells contain half the amount of DNA of C cells, which has led to the argument that these cell types may be alternate life cycle phases with the S cells forming the gametic phase (Green *et al.*, 1996; Billiard, 1994). However, this has not been proven and the functions of different cell types remain a mystery.

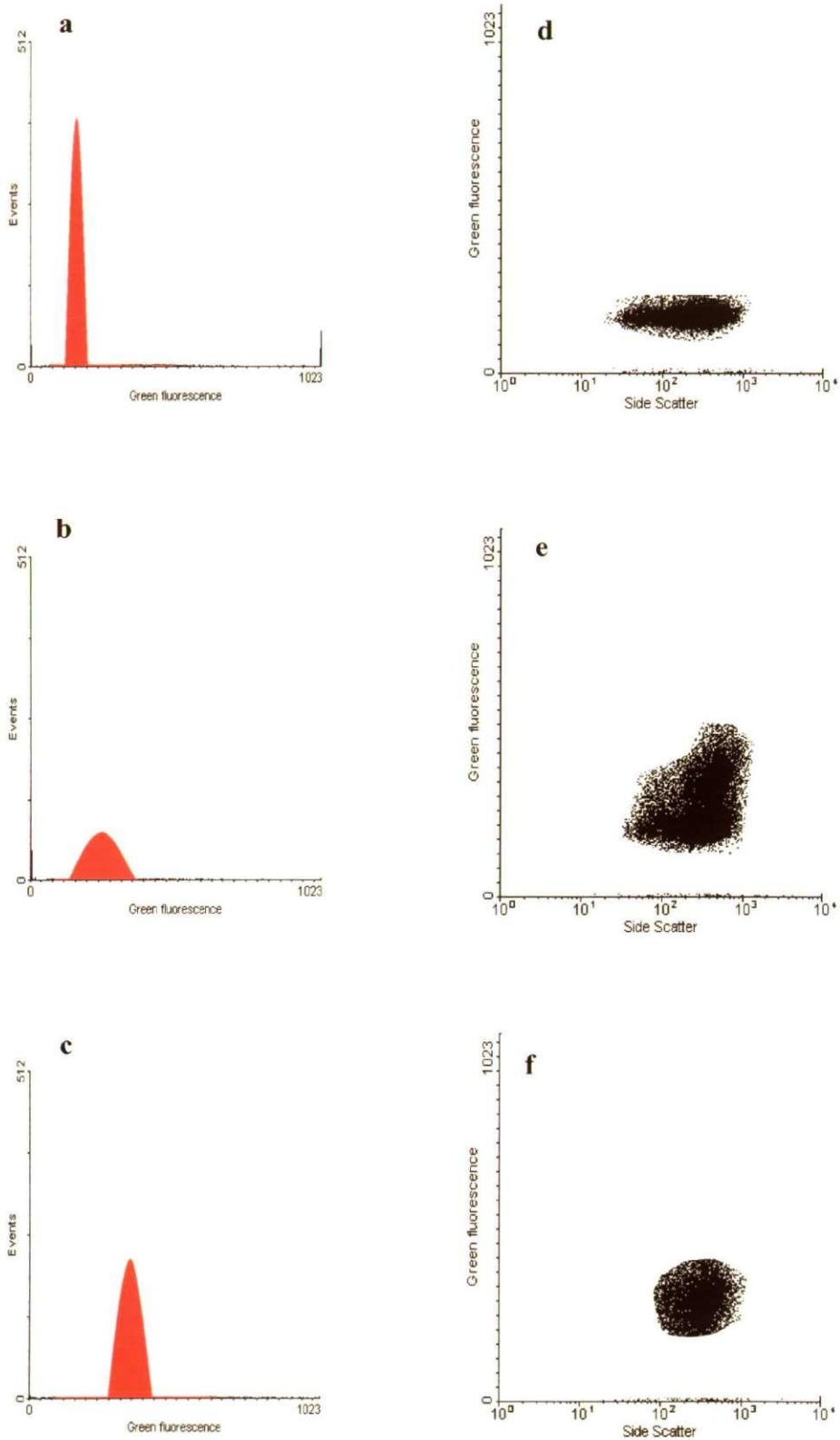


Figure 1.4 Flow cytometry plots illustrating *E. huxleyi* CCMP1516 at the three different phases of the cell cycle. Frequency histograms of green fluorescence at G1 (**a**), S (**b**) and G2 + M (**c**) phases. Corresponding scatter plots of side scatter vs green fluorescence at G1 (**d**), S (**e**) and G2 + M (**f**) phases.

1.5. Viruses

Viruses are sub microscopic intracellular parasites. They are infectious particles which consist of nucleic acids (DNA or RNA) which are enclosed by a protein layer (capsid). They are unable to carry out replication or any metabolic processes; for this they depend on a host cell. Infection occurs through interaction with the host cell surface membrane which permits the virus to insert its nucleic acid into the host cell. Once inside the host, the virus is able to exert control over the host metabolism and reproduce. There are two principal mechanisms for virus reproduction; the lytic cycle or the lysogenic cycle. The lytic cycle occurs when infected cells are destroyed or burst open in order for the virus progeny to be released; in the lysogenic cycle, the virus genetic material is incorporated into the host genome and the host replicates as normal, carrying a copy of the virus genome with it. Lysogenic cells can revert to lysis, although the trigger for this in natural environments is unknown.

1.5.1. Viruses in Phytoplankton

In recent decades, aquatic viruses have been increasingly studied and their important role within aquatic systems is becoming ever more apparent (for example Larsen *et al.*, 2001). Bergh *et al.* (1989) reported the high number of viruses found in various aquatic environments suggested that they have a greater ecological role than previously thought. Cochran *et al.* (1998) reported similar virus numbers with variation between marine systems: 10^4 ml⁻¹ in oligotrophic and deep-sea habitats up to 10^8 ml⁻¹ in coastal and estuarine habitats. Increasing research into marine virology has revealed that viruses are significant components of marine plankton ecosystems and they have important influences on several fundamental actions. This in turn has impacts on other system components: the flow of dissolved organic matter (Middelboe *et al.*, 2003; Riemann & Middelboe, 2002), nutrients (Wilhelm & Suttle, 1999) and DMS dynamics

(Hill *et al.*, 1998). Through these impacts, a feedback mechanism occurs which allows the coexistence of phytoplankton and virus populations; the infection rate falls as the abundance of the host is reduced by earlier infections, virus numbers then fall, but nutrients are present at an increased level following lysis of the original host population, thus allowing the remaining hosts to reproduce and become abundant again (Thyrhaug *et al.*, 2003). Whilst being a major cause of algal demise, viruses also maintain the future algal populations.

A number of anti-viral mechanisms in phytoplankton have been proposed; however most are without strong supporting evidence for or against. Sinking rates increase in infected *Heterosigma akashiwo* and this may act to protect remaining host cells as the infected cell sinks out of the photic zone taking the virus progeny with them (Brussaard, 2004). The process of apoptosis is another possible mechanism preventing viruses reproducing: when a host cell detects infection it dies instantly, thus protecting the remaining population from further virus release. It is not known to what extent this is employed in phytoplankton (Brussaard, 2004). These mechanisms are altruistic and act to protect the population rather than individual cells. Murray (1995) suggests that healthy phytoplankton exude dissolved organic matter in an attempt to support bacterial growth around them which acts as a virucidal agent. Murray and Jackson (1992) discuss the role of size and motility on virus host encounters and conclude that large, non-motile phytoplankton may be less susceptible to virus encounter than smaller motile phytoplankton. These morphological differences have also been suggested to provide intra-species differences in vulnerability. *E. huxleyi* has different morphotypes (section 1.4) and these are suggested to alter the infectivity of the host. Scaly and naked cells appear to suffer greater levels of infectivity than lithed cells (scaley (Brussaard *et al.*, 1996; Bratbak *et al.*, 1995) and naked (van Bleijswijk *et al.*, 1996)).

Following lysis, new virus progeny are at their most vulnerable. They are free particles in the water column whilst searching for a host and are vulnerable to loss via a number of mechanisms including grazing by protozoa and damage through ultra violet radiation (UVR). UVR causes damage to the genetic material of the viruses, causing them to be unable to commandeer a host and therefore are unable to replicate (Jeffrey *et al.*, 2000). In the photic zone of the water column, high levels of UV light are frequent, and are certainly encountered during bloom conditions (Nanninga and Tyrrell, 1996). In order to counteract these losses and maintain the population (which are known to be relatively stable over seasonal scales (Wommack and Colwell, 2000)), they must maintain a high input of progeny; Wommack and Colwell (2000) discuss the viral lysis rates required to maintain virus population from a variety of locations. This revealed an average of 2 – 24% of the bacterioplankton population needed to be lysed per hour to maintain a stable virus population. This high level of host lysis explains how viruses are capable of having a large impact on microbial system dynamics.

1.5.2. Viruses in *Emiliana huxleyi* Blooms

Virus specific to *E. huxleyi* were first observed in 1974 and their identity was confirmed by Bratbak *et al.* in 1996. A number of other isolates have since been discovered (Castberg *et al.*, 2002; Wilson *et al.*, 2002b). Further studies have started to reveal the effects of these viruses on *E. huxleyi* in both laboratory and natural systems. *E. huxleyi* viruses (EhV) are approximately 170nm – 190nm with icosahedral symmetry, they have double stranded DNA and are lytic (Schroeder *et al.*, 2002). Several isolates are known (Schroeder *et al.*, 2002) which have been collected from waters off Plymouth, UK (Wilson *et al.*, 2002b) and Bergen, Norway (Castberg *et al.*, 2002). These viruses have been classified in a new genus (*Coccolithovirus*) within the family *Phycodnaviridae* which includes algal viruses. Ten virus isolates are recorded

by Schroeder *et al.*, (2002) which all have similar host ranges when inoculated to a number of host strains. Two of these strains were found to be resistant to infection by these isolates.

There are records of a link between the collapse of *E. huxleyi* blooms and the presence of large virus-like particles (LVLPs) since before EhV were identified (Bratbak *et al.*, 1993). Research in this area found that these LVLPs can be a major factor in bloom collapse: Brussaard *et al.* (1996) reported viral lysis to be an important factor controlling a natural *E. huxleyi* bloom in the North Sea and Wilson *et al.* (2002b) concluded that EhV were responsible for the collapse of a naturally occurring bloom in the English Channel. Under controlled conditions, Castberg *et al.* (2001) showed mortality of *E. huxleyi* was due to viral attack; they monitored other conditions such as grazers and nutrient levels which could be alternative mortality factors in an *E. huxleyi* bloom however none of these factors were found to be at lethal levels.

The activity of the viruses in the blooms is also beginning to be deciphered. Brussaard *et al.* (1996) discusses the role of viruses in microbial loop dynamics: the input of organic carbon from viral lysis is an important resource for bacteria. Schroeder *et al.* (2003) revealed the presence of different phenotypes during the stages of a bloom with only 3 being likely to have terminated the bloom. Jacquet *et al.* (2002) found virus release to vary throughout the day and night and attributed this to a light dependent virus release with virus numbers reducing in the second part of the day. This corresponds with the vulnerability of viruses to UVR damage; by releasing less during the higher UVR part of the day, less viruses are lost through environmental damage therefore making virus release more efficient.

The intricate relationship between host and virus is beginning to be understood but there are many questions which remain unanswered regarding this system.

1.6. Virus Effects on Hosts

The effects of cell cycle phase at infection were studied in *Phaeocystis pouchetti* and *Pyramimonas orientalis* by Thyrhaug *et al.*, (2002). Cultures were infected at four times during the cell cycle and then monitored them for 30 hours. Contrasting results were found for the two species; in *P. pouchetti* virus production was independent of cell cycle. However, in *P. orientalis* there was an eight-fold variation in the numbers of viruses released in the different cultures. Thyrhaug *et al.* (2002) could not conclude from their results whether this difference was directly due to the cell cycle variation, or another factor which was linked to the light:dark cycle.

Observing this situation from the alternative view is the effects of infection on the host rather than the virus success. Work carried out on a number of other virus groups has led to some interesting conclusions regarding the cell cycle progression in infected hosts. Song *et al.*, (2000) found that cells infected with the herpes simplex virus (HSV) during the G1 phase, remained in the G1 phase. The benefit of this function to either host or virus is unknown. Successful infection occurs independently of host cell cycle phase at infection, however this discovery mirrored the actions of other herpesviruses which also blocked their hosts if infected during the G1 phase.

1.7. Overall Summary

This review provides the background to this project. The following chapters will detail the materials and methods used to test the aims, tests of the cell cycle during the project and the changes which were recorded in the ploidy levels of the *E. huxleyi* culture, the results of the experiments, followed by the discussion, conclusions and from this some suggestions for further work.

2. Materials and Methods

2.1. Materials

2.1.1. *f/2*

f/2 media was prepared as in Guillard & Ryther 1962 and Guillard 1975 (<http://ccmp.bigelow.org>). The compounds listed in table 2.1 were added to sterile filtered (30kDa) seawater to a final volume of 1L. Seawater was collected from Station L4 (50°15'N 04°13'W) south of Plymouth, UK in the English Channel on a number of occasions during the project.

Quantity	Compound	Stock Solution	Molar Concentration in Final Medium
1 mL	NaNO ₃	75 g/L dH ₂ O	8.83 x 10 ⁻⁴ M
1 mL	NaH ₂ PO ₄ · H ₂ O	5 g/L dH ₂ O	3.63 x 10 ⁻⁵ M
1 mL	<i>f/2</i> trace metal solution	(see table 2.2)	-
0.5 mL	<i>f/2</i> vitamin solution	(see table 2.3)	-

Table 2.1 Compounds required for *f/2* media.

Quantity	Compound	Stock Solution	Molar Concentration in Final Medium
3.15 g	FeCl ₃ · 6H ₂ O	-	1 x 10 ⁻⁵ M
4.36 g	Na ₂ EDTA · 2H ₂ O	-	1 x 10 ⁻⁵ M
1 mL	CuSO ₄ · 5H ₂ O	9.8 g/L dH ₂ O	4 x 10 ⁻⁸ M
1 mL	Na ₂ MoO ₄ · 2H ₂ O	6.3 g/L dH ₂ O	3 x 10 ⁻⁸ M
1 mL	ZnSO ₄ · 7H ₂ O	22.0 g/L dH ₂ O	8 x 10 ⁻⁸ M
1 mL	CoCl ₂ · 6H ₂ O	10.0 g/L dH ₂ O	5 x 10 ⁻⁸ M
1 mL	MnCl ₂ · 4H ₂ O	180.0 g/L dH ₂ O	9 x 10 ⁻⁷ M

Table 2.2 Compounds required for *f/2* trace metal solution. Made to a final volume of 1L dH₂O and autoclaved.

Quantity	Compound	Stock Solution	Molar Concentration in Final Medium
1 mL	Vitamin B ₁₂ (cyanocobalamin)	1.0 g/L dH ₂ O	1 x 10 ⁻¹⁰ M
10 mL	Biotin	0.1 g/L dH ₂ O	2 x 10 ⁻⁹ M
200 mg	Thiamine · HCl	-	3 x 10 ⁻⁷ M

Table 2.3 Compounds required for *f/2* vitamin solution. Made to a final volume of 1L dH₂O and autoclaved.

2.1.2. Buffers and Solutions

Buffer or Solution	Constituents	Manufacturer
Tris-EDTA buffer (TE)	10mM Tris at 10ml ⁻¹ L, 1mM EDTA at 2ml ⁻¹ L, pH 7.6	
SYBR Green I	Working stock made fresh to 1:100 or 1:1000 dilution	Molecular Probes
Gluteraldehyde	50% EM grade	Sigma
RNAseA	Final concentration of 0.1mg per 1ml sample	Sigma

Table 2.4 Buffers and solutions used during various experiments

2.1.3. Microalgae Cultures

The microalgal host used in this study was *E. huxleyi* strain CCMP1516 (<http://ccmp.bigelow.org>), obtained from collections at the Marine Biological Association of the UK. The algae were maintained in *f/2* (see Table 2.1) at 15°C in a Sanyo MLR-350 incubator with a light:dark cycle of 16:8, during the light phase 1 of the Sanyo FL4OSS strip tubes were it, on 3 sides of the incubator. Cultures were sub cultured when reaching 5 x 10⁵ cells per ml. Cell numbers were monitored under a light microscope using a haemocytometer with approximately 10µl of culture. The algal culture was axenic.

2.1.4. Viruses

Virus lysate was obtained by adding virus strain EhV86 (Wilson *et al.*, 2002b) from the Marine Biological Association of the UK to exponentially growing hosts in *f/2* medium (Guillard, 1975) to a multiplicity of infection of approximately 1. Lysis of the host culture usually occurred within a week and stock virus was obtained by filtering using a Nalgene bottle top filter unit with a 0.45µm filter (Pallgelman Supor) to remove cell debris. The filtrate was stored at 4°C in the dark prior to use. The virus lysate was axenic.

2.2. Methods

2.2.1. Analytical Flow Cytometry

All analyses were performed with a Becton Dickinson FACSort™ flow cytometer equipped with an air-cooled 15mW laser providing 488nm light with a standard filter set-up which measured chlorophyll fluorescence (> 650 nm), phycoerytherin fluorescence (585nm ±21nm), forward scatter (light scattered in the same plane as the laser beam) and side scatter (light scattered at ninety degrees to the plane of the vertically polarised laser). Measurements of side scatter and green fluorescence were made using CELLQuest™ software (Becton Dickinson) with log amplification on a four-decade scale. Data analysis was carried out using WinMDI 2.8 software (Joseph Trotter – freely available from <http://facs.scripps.edu>). Scatter-plots of side-scatter vs green fluorescence and side-scatter vs red fluorescence were used to analyse virus and host numbers, respectively.

2.2.1.1. Virus Enumeration

Thawed virus samples were diluted to 1:10, 1:100 or 1:1000 (depending on virus numbers in sample) in TE buffer (10mM Tris-HCl pH 7.5, 1mM EDTA) (pre-filtered through a 50kDa VivaFlow 50 ‘flip-flow’ system (Satorius) then autoclaved) to a

volume of 990 μ l (10 μ l of stain is added so total volume is 1ml). Diluted samples were stained with SYBR Green I (Molecular Probes) at a final concentration of 10^{-4} of the commercial stock solution and heated at 80°C for 12 minutes in the dark. Samples were run for 2 minutes at an average flow rate of 23 μ l min $^{-1}$ with the discriminator set to green fluorescence (for accuracy, flow rate was measured for 15 to 30 minutes before and after each session of analysis). Data acquisition was triggered on green fluorescence and the detection threshold was adjusted to cut out most of the instrument noise from the blank. Figure 2.1 shows a typical plot of EhV.

2.2.1.2. Host Enumeration

For enumeration of live host counts during experiments undiluted and unstained fresh samples were run for 3 minutes at an average flow rate of 17.1 μ l min $^{-1}$ with the discriminator set to red fluorescence. Figure 2.2 shows a typical plot of *E. huxleyi* strain CCMP1516.

2.2.1.3. Cell Cycle Analysis

Cell cycle analysis involved measuring the DNA content of the cells to identify if cells were in the growth (G1), DNA synthesis (S) or replication phase (G2 + M). This involved more detailed analysis on the flow cytometer: scatter plots of side scatter vs red fluorescence, side scatter vs green fluorescence and green fluorescence vs red fluorescence and a histogram of green fluorescence frequency were produced to allow for an accurate analysis. Figure 2.3 shows a typical cell cycle analysis of *E. huxleyi* strain CCMP 1516.

Before analysing, RNaseA was added to defrosted samples at a concentration of 0.1mg per ml and incubated at 37°C for 2 hours. Undiluted samples were then stained with SYBR Green at a final concentration of 10^{-3} for 30 minutes at room temperature

and analysed by flow cytometry. Samples were run until 20 000 particles in the gated region of *E. huxleyi* had been recorded. Samples took between 1:30 and 5:00 minutes to register this number of cells.

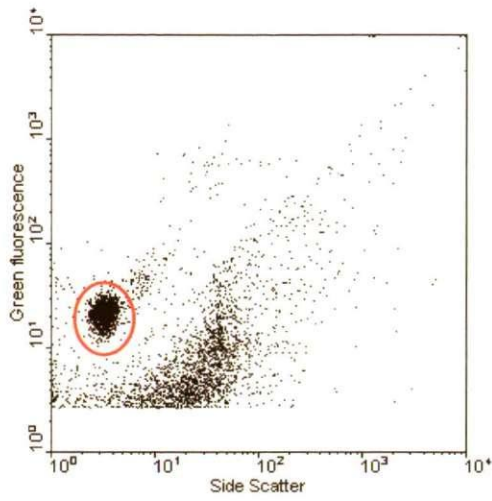


Figure 2.1 Typical plot of *EhV* 86

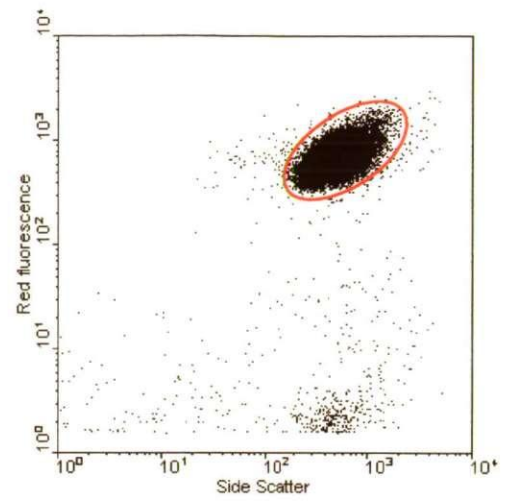


Figure 2.2 Typical plot of live *E. huxleyi* strain CCMP1516

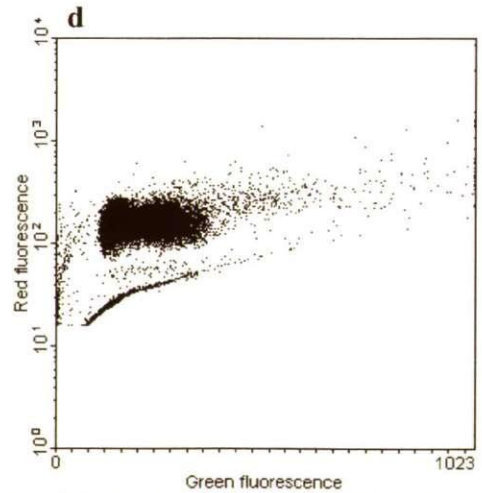
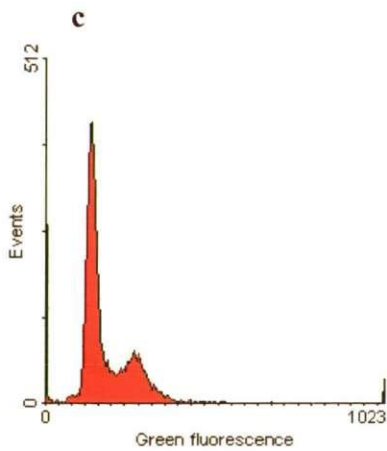
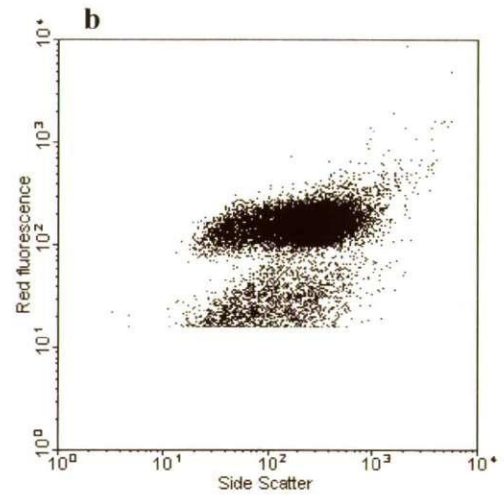
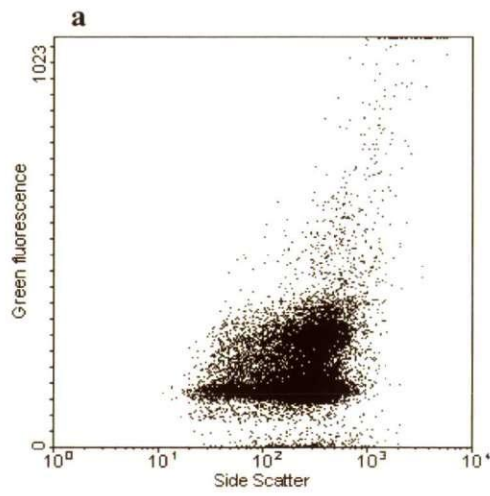


Figure 2.3 Typical plots from cell cycle analysis of *E. huxleyi* strain CCMP1516. **a** green fluorescence vs side scatter, **b** red fluorescence vs side scatter, **c** green fluorescence frequency histogram and **d** red fluorescence vs green fluorescence

2.2.2. Plaque Assays

2.2.2.1. Preparations

Base agar plates were prepared in a few days in advance using 1.5% agarose *f*/2 media and were stored at 4°C once set. 500ml agarose made approximately 30 plates.

Concentrated *E. huxleyi* was prepared within 18 hours of the experiment starting. Aliquots of concentrated uninfected *E. huxleyi* cells were sourced from the original large culture which was divided into 50ml volumes and centrifuged using a benchtop eppendorf centrifuge (model 5810 R) for 5 minutes at 5000rpm at 4°C. The supernatant was removed and cells were resuspended in 1ml of *f*/2. This was kept incubated at 15°C until required during the experiments.

2.2.2.2. Samples

Plaque assays were taken two hours after infection (experiment one) and two and four hours after infection (experiment two).

Samples comprised of six 1.5ml aliquots of the infected culture. Samples were 'washed' to remove any free viruses: they were centrifuged at 14000rpm for 1 minute. The supernatant was removed and the pellet of *E. huxleyi* cells was resuspended in 1.5ml of *f*/2. This was repeated twice. On the final wash, the pellet was resuspended in 1ml of concentrated *E. huxleyi* (section 2.2.2.1). Samples were then incubated for two hours at 15°C.

Following the two hour incubation period, the samples were split and added *E. huxleyi* cells in differing volumes to produce five concentrations of infected sample: undiluted, 0.5, 10^{-1} , 10^{-2} and 10^{-3} .

Agarose for the top layer was prepared during the two hour incubation period and was a 0.4% agarose *f*/2 mixture. This mixture was then kept in a 40°C water bath to maintain the agarose at the minimum temperature and also remaining liquid. Each

sample was vortexed briefly with 3ml of 0.4% agarose and immediately poured onto the prepared base plates.

Plates were incubated at 15°C and observed after two weeks.

2.2.3. Infection Experiments

To test whether virus production is host cell cycle dependent, 4L of exponentially growing cultures were mixed and split into 4 x 1l cultures. These were infected with 2ml of virus stock at G1 phase (T = 0 h, 4.5 hours into the light phase), S phase (T = 8 h, 12.5 hours into the light phase) and G2 + M phase (T = 14 h, 2.5 hours into the dark phase). The initial multiplicity of infection was 1. In the second experiment, cultures were split and infections began with the G2 + M phase (T = 0 h) followed by G1 phase (T = 10 h) and S phase (T = 18 h).

In each experiment, the following samples were taken once every 2 h for 48 h: virus, cell cycle and host number. All samples were fixed in 0.5% glutaraldehyde and refrigerated at 4°C for 20 minutes. Samples were then snap frozen in liquid nitrogen and stored at -80°C.

After the final time point, twice daily samples were taken at 21:00 and 09:00 to record the collapse of the host populations. This occurred for an additional 4 time points.

2.2.3.1. Virus Samples

Virus samples were taken by centrifuging 1.5ml culture samples at 14 000rpm for 2 minutes and removing 1ml of supernatant which was then fixed. These were taken in triplicate in each of the infected cultures beginning at the time of infection.

2.2.3.2. Cell Cycle Samples

Cell cycle samples were taken in single samples of 1ml. These were taken from all cultures at every time point from the first infection.

2.2.3.3. Host Numbers

Host numbers samples were taken in single samples of 2ml which were immediately analysed using flow cytometry. These were taken from all cultures at every time point from the first infection.

2.2.4. Adsorption Assay

The first adsorption experiments were run parallel to the infection experiments. Virus samples of the newly infected culture were taken in triplicate every 20 minutes for the 2 h after infection and fixed. Host numbers and cell cycle samples were taken as part of the infection experiment. Plaque assays were produced for the infected culture 2 hours after each infection.

The second adsorption experiment involved a more intense sampling programme and was run separately to the second infection experiment. Infection points were at the same times as previously, beginning with the G2 + M phase (T = 0 h) followed by G1 phase (T = 10 h) and S phase (T = 18 h). Virus counts were taken and fixed in triplicate every 10 minutes for the 2 hours following infection. Triplicate plaque assays for the infected cultures were produced 2 hours and 4 hours after each infection. Cell cycle and host numbers were recorded as previously at 0, 2 and 4 hours after infection.

2.2.5. Cell Cycle Tests

During the project it was necessary to investigate the cell cycle and ensure that the cultures were synchronised with their light:dark cycle. Cell cycle samples were

taken on two occasions: first at infection times (17:00, 01:00 and 07:00) and then at more frequent intervals, but including the infection times (17:00, 21:00, 01:00, 04:00, 07:00, 10:00, 13:00). 1ml samples were taken in triplicate and fixed and analysed as before.

3. Cell Cycle Tests and Culture Ploidy

3.1. Introduction

The analysis of the host cell cycle was a key task during this project. As described in section 2.2.1.3, flow cytometry was used to measure the DNA levels in the host cells. The results in this section are from two tests of the cell cycle which occurred following a change of laboratories. During a move between laboratories, the timings of the light:dark cycle of the host culture incubators were changed. They remained on a 16:8 hour cycle but the light phase ended 4 hours earlier than under the original conditions. It was decided that in order to repeat the first cell cycle experiment, it would be preferable for the cultures to be on the original light:dark cycle and therefore the cultures were moved to an incubator with these timings. It was necessary to ensure that the cell cycle had resynchronised with their new timings before beginning any experimental work so the cell cycle was sampled (section 2.2.5).

By measuring the green fluorescence of 20 000 host cells, it is possible to get a measure of the amount of DNA in the cells at various time points. From this a histogram of the frequencies of the DNA levels in each of the cells can be plotted and used to determine the cell-cycle stage of the cells. For example, G1 phase has a large peak at a low measure of green fluorescence which represents the cells containing a single copy of their DNA (fig. 1.4). As the cells move into the S phase (DNA synthesis) the green fluorescence increases and the G1 peak becomes smaller and starts to shift to the right as the DNA content per cell increases. The final phase is G2 + M; cells contain two copies of their genomic DNA ($4n$) and here have double the green fluorescence compared to the G1 phase, the peak on the histogram has moved further to the right with a small G1 peak remaining which represents the cells which have already divided.

Parallel to the histogram plots, scatter plots of side scatter vs green fluorescence allow us to view the populations of cells as they shift between phases (fig. 1.4). This is

valuable data, particularly if the histogram data do not initially appear to fit the predicted pattern which will happen if there is a range of ploidy levels in the same culture. The aim of this chapter is to investigate ploidy levels in *E. huxleyi* strain CCMP1516 and accurately determine timing of cell cycle stages.

3.2. Results

An initial investigation of the cell cycle following a change in the light:dark cycle timing suggested that the *E. huxleyi* cultures were not synchronised with the light:dark cycle (fig. 3.1). The 17:00 sample appeared to show a G1 phase, as expected, however the sample we expected to be in S phase (01:00) had a wide single peak which looked like it was in the G2 + M phase. Finally, the sample we expected to be in G2 + M phase (07:00) had actually already shifted to G1 phase. This result suggested that cell cycle was out of phase with the light: dark cycle.

After a further three weeks, the cell cycle was re-analysed. During this three week period, subculturing was carried out more often in mid-exponential stage of the growth curve (previously, sub-culturing was conducted in the late exponential stage) which allowed the cultures to adjust to new light:dark conditions quicker.

The histograms from the second experiment appeared to show that the culture had in fact become less synchronised with the new light:dark cycle than the initial experiment (above) since the histograms showed no obvious pattern to suggest what phase the cells were in (fig. 3.2). However, scatter plots of side scatter vs green fluorescence (fig. 3.1 d - f) suggested there were changes within the host population that were obscuring the histogram results. It appears that there are a number of populations within the scatter plots (fig. 3.3) which had increasing mean green fluorescence signals of approximately double that of the previous group. The changing numbers of these populations can be followed and show the same pattern as would be predicted if the cell

cycle was synchronised with the light:dark cycle: from the 17:00 h samples, these groups can be traced to increase through an S phase to a level of higher DNA content (G2 + M phase) and then back to a G1 phase with the original green fluorescence signal (fig. 3.2).

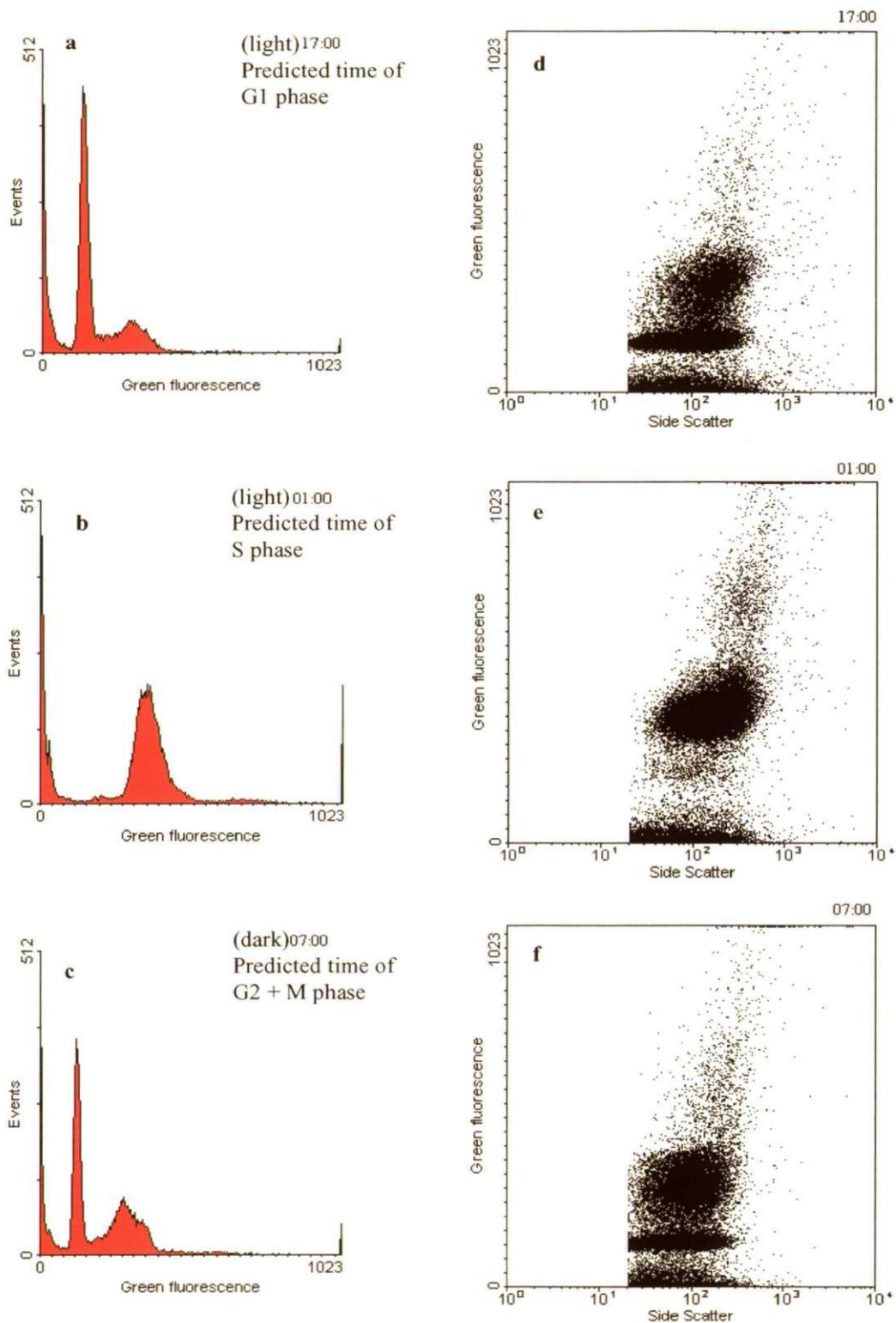


Figure 3.1 Cell Cycle images of *E. huxleyi* strain CCMP1516 from initial cell cycle test following shift in light:dark growth timing. Histograms of green fluorescence frequencies and scatter plots of side scatter vs green fluorescence at times 17:00 predicted G1 Phase (**a, d**), 01:00 predicted S Phase (**b, e**) and 07:00 predicted G2 + M Phase, (**c, f**). During the light:dark cycle the light was switched on at 1230hrs and switched off at 0430hrs (16 hours light); hence, dark phase occurred between 0430hrs and 1230hrs (8 hours dark).

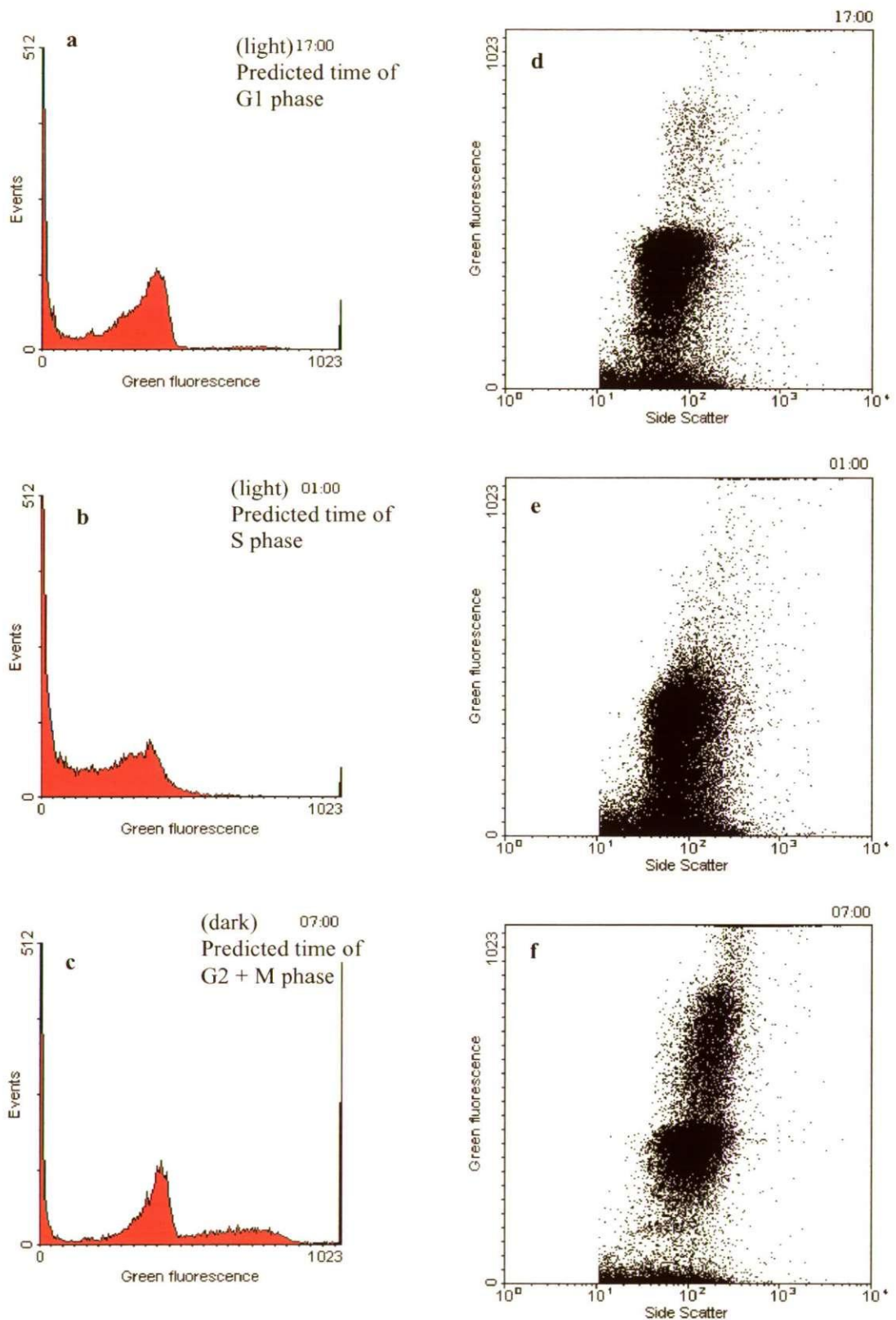


Figure 3.2 Cell Cycle images of *E. huxleyi* strain CCMP1516 from second cell cycle test following shift in light:dark growth timing. Histograms of green fluorescence frequencies and scatter plots of side scatter vs green fluorescence at times 17:00 predicted G1 Phase (**a, d**), 01:00 predicted S Phase (**b, e**) and 07:00 predicted G2 + M Phase, (**c, f**). During the light:dark cycle the light was switched on at 1230hrs and switched off at 0430hrs (16 hours light); hence, dark phase occurred between 0430hrs and 1230hrs (8 hours dark).

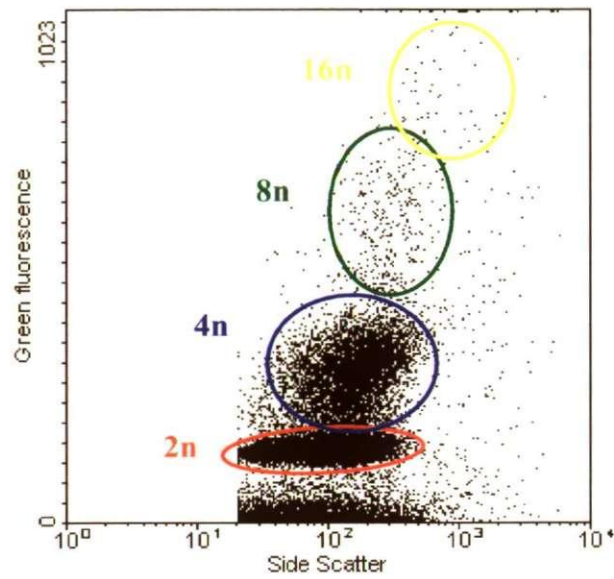


Figure 3.3 Populations of increasing DNA content observed in *E. huxleyi* strain CCMP1516 during G1 phase indicating populations of cells at different ploidy levels, 2n – 16n.

3.3. Discussion

The changes found in this culture illustrate that the cell cycle has become synchronised with the required light:dark cycle, but also that the population has split into a number of increased ploidy sub-populations. The increased green fluorescence signal suggests that the original diploid $2n$ culture, to having a $4n$ and $8n$ population present, as well as a residual $2n$ population (fig. 3.2 d – f). It is also possible that there are other populations with even greater quantities of DNA present as these are above the detection limits of this sample so would not have been recorded.

This is an important change in view of this project as it alters the magnitude of host activity during the cell division phase when the host is most vital to the virus. If the host is replicating twice as much DNA (or 4 times as much) will this have an impact on the division of the viruses?

When looking back on the first cell cycle test, it is now possible to see that the cultures had synchronised with the intended light: dark cycle but the presence of the multiple ploidy groups had made the histograms appear unsynchronised. This is because, in a $2n$ population, as cells increase their DNA content during the $G2 + M$ phase, the peak of DNA content shows the doubling. If there is a $4n$ population in the culture, this population will occupy the double peak during the $G1$ phase, making it appear as if there is a $2n$ population which is not in the normal cell cycle.

When the results of the first cell cycle test were reanalysed (fig. 3.1), it was found that the cultures had synchronised with the new light:dark cycle. The scatter plots of green fluorescence vs side scatter made it clear that there are several populations present. When analysing the cell cycle using regions around the different ploidy populations on the scatter plots, it is again possible to follow the cell cycle changes of each population as they respond as predicted under the original light:dark settings.

It is unknown whether these results may alter the host:virus relationship when the experiments were repeated, however it was decided to continue with the multi-ploidy culture. Van Bleijsweijk *et al.*, (1996) recorded the strong control of the cell cycle timings in various cultures: laboratory and natural cultures, various morphotypes (including haploid and diploid cells) and under different temperature, light and nutrient conditions. In all these cultures the key cell cycle events occurred at the same time, and although none of these cultures had larger ploidy levels than the diploid culture, it is clear from our results that increased ploidy in *E. huxleyi* strain CCMP1516 does not have an effect on the timings of the cell cycle. This point is supported by the results that cultures during the second experiment (fig. 3.2) had fallen into time with the predicted cell cycle.

Such changes in ploidy levels within *E. huxleyi* cultures have never previously been reported. However, there are recordings of changes within *E. huxleyi* cultures occurring between cell types. Paasche (2002) describes how senescent cultures of type C cells (section 1.3.2) can give rise to N or S type cells, and states that this can be avoided by frequent transfer to new growth medium. This is the opposite of what has occurred in our cultures: they have been cultured at frequent intervals for several months and the DNA content has increased, whereas Paasche (2002) reports senescent cultures resulting in a population with reduced DNA.

4. Results

4.1. Introduction

During this project four experiments were completed. These included two infection experiments which each involved infecting three *E. huxleyi* cultures at different points in the cell cycle, then monitoring virus numbers, host numbers and cell cycle phase every two hours for 48 hours. These two experiments differed in their starting times: the first experiment was started with infection during the G1 phase (17:00) and the second experiment was started with infection during the G2 + M phase infection (07:00) (fig. 4.1). The aim of the experiment was to determine if the efficiency of infection was influenced by what cell cycle phase the cells were in during initial virus adsorption.

The second set of experiments was the adsorption experiments where three cultures were infected as in the infection experiments (above), but the sampling was focussed on the initial hours after the infection. Virus numbers were taken every 20 minutes for 2 hours in the first experiment and every 10 minutes in the second. Plaque assays were produced 2 hours after infection in the first experiment and 2 and 4 hours after infection in the second. The first adsorption experiment was run simultaneously with the first infection experiment whereas the second was run separately due to the increased sampling intensity.

This chapter will describe the results from the adsorption and infection experiments.

4.2. Infection Experiments

4.2.1. Cell Cycle

4.2.1.1. Cell Cycle at Infection Points

Samples were taken to ensure that the cultures were in the correct stages of the cell cycle at the points of infection. Figure 4.2 shows the images taken at the infection points and show the cultures to be in the correct phases in all cultures of both experiments and also that they were synchronised with the control culture (marked with red boxes in fig. 4.2).

4.2.1.2. Cell Cycle During Infection

During both experiments, cell cycle was monitored. This was to ensure that the cultures were in the correct phase when they were infected and to monitor whether any changes in the cell cycle took place in the infected cultures. The results are shown for key time points during the 48 hours of the experiments. When comparing the two experiments, it is possible to see that the control cultures of the two experiments were very similar which is a measure of the replication between the experiments.

The presence of multi ploidy sub-populations in the cultures and the viruses within the hosts may potentially confound these results by changing the DNA signature of the hosts. However, following the time series of the cell cycle histograms, and comparing with the control culture, it is possible to see a pattern. The infected cultures lose their cell cycle phasing; the control culture retains its cell cycle throughout both experiments (fig. 4.2). Cultures show a gradual reduction in their similarity to the control culture and a move towards a single, wide based peak with the mean green fluorescence slightly above that of the typical G1 phase peak (table 4.1).

	G1 Infected	S Infected	G2 + M Infected
Culture deviates from Control in IE 1	24	24	18
Culture deviates from Control in IE 2	26	26	26
Single peak appears in IE 1	32	40*	34
Single peak appears in IE 2	32	-	40

Table 4.1 Hours after infection that changes in the cell cycle occur. IE 1 = infection experiment one, IE 2 = infection experiment two. *The 30 hour sample is missing in this culture, so this result may be later than the actual time of the peak occurring.

In infection experiment two, the samples taken at time points between those shown in figure 4.2 were analysed and it was possible to get a more precise time of when changes occurred. In infection experiment one, only the times shown were analysed which means that the results recorded may be later than the time the changes occurred.

Figure 4.3 shows the variation in the 2n and 4n populations in host population during infection experiment two. As described in section 3.1, the use of the region statistics taken from the scatter plots can allow for further analysis of the cell cycle data. From these graphs, it is possible to see the division cycle occurring over the first 24 hours with a similar cycle in all four cultures. In the control culture (fig. 4.3a) this cycle repeats (with the exception of an anomalous result at 15:00 on the second day), but in the infected cultures (fig. 4.3 b-d) this is interrupted in the later hours of the experiment. This reiterates the changes noted in fig. 4.2.

4.2.2. Host Numbers

During the first 24 hours of both experiments, all cultures show an increase of host numbers during the dark phase as they divide. Division is followed by a slight decrease in cell numbers (fig. 4.4). The control cultures continue to show a healthy division cycle for the remainder of both experiments, whereas the infected cultures all collapse by the end of the experiment. The onset of culture collapse varies between the cultures and experiments (table 4.2). In experiment one, complete lysis of all cultures occurred four days after infection. In experiment two, the G1 and S phase collapse on day five and the G2 + M culture collapses on day four (data not shown). The control culture reaches a plateau on the day the infected cultures collapse and remains healthy after this point. This indicates that the virus infection caused the cultures to collapse.

	G1 phase Infected	S phase Infected	G2 + M phase Infected
Experiment 1	48	56	30
Experiment 2	52	60	48

Table 4.2 Number of hours after each infection that each culture begins to crash in each experiment.

4.2.3. Virus Numbers

Virus numbers from both experiments show an initial drop in all three cultures after the point of infection (fig. 4.5). The drop lasts between 4 and 6 hours in the first experiment (fig. 4.5a) and between 4 and 10 hours in the second experiment (fig. 4.5b). After this point, virus numbers increase at a near constant rate until and eventually plateau 50 to 60 hours after infection (the beginning of the plateau in the G2 + M culture during experiment is visible in figure 4.5b; data for the other cultures is not shown). In

the first experiment, there was a clear reduction in the rate of virus release during the dark stages of the light:dark cycle in cultures which were past the initial adsorption of viruses (fig.4.5a). In the second experiment, there was not a clear plateau but there is a decrease in the release rate during the dark stage and there is overlap in the error bars during the dark phase which is rarely seen in the light phase (fig. 4.5b). There is a difference in the adsorption time in the cultures: viruses added during G1 phase adsorbed for 4 hours prior to the onset of virus release, compared to between 6 – 10 hours in S and G2 + M phase in both experiments.

4.3. Adsorption Experiments

The plaque assays from the first experiment revealed a large difference between the infection successes of the cultures (fig. 4.6). The number of plaques observed in the G2 + M infected culture after two hours of adsorption is three times greater than during the G1 or S phase infections. This pattern is visible in the 10^{-1} and the 0.5 dilutions but was beyond the limit of detection in the higher dilutions (10^{-2} and 10^{-3}). In the more concentrated assays, plaques overlapped and therefore lead to inaccurate numbers of plaques being recorded, hence these results were discarded.

The plaque assays in the second experiment yielded no results: no plaques were observed in any dilutions of any of the cultures.

The virus numbers during the two hour adsorption phase did not reveal a significant difference in the adsorption rate of the cultures in either experiment (fig. 4.7). There is a clear adsorption occurring (this is also seen in fig. 4.5 in the first hours after each infection) as the numbers of viruses decreases overall during the two hours. There is a slight difference in the shape of the curves of virus loss between the cultures. In infection experiment one, the G2 + M phase seems to have a slower but more stable rate of adsorption compared to a more rapid virus loss in the first hour and a reduced rate of

virus loss during the second hour as seen in the G1 and S phase cultures. In infection experiment two, a similar pattern is seen, with the exception of the S phase which shows no pattern. All these differences are statistically insignificant due to the large amount of variation, and the patterns are not a reliable interpretation.

It is difficult to construe any patterns in the G2 + M phase owing to the anomalous samples in the first record of the assay when the virus numbers appear to increase within the first 20 minutes of infection. This result is likely to be a sampling error despite efforts to maintain identical sampling procedures between cultures. It is unlikely that a virus release had occurred in the first 20 minutes of the infection which would be large enough to counteract the adsorption that would have been taking place. The numbers of viruses during the initial adsorption phases were at the lowest sensitivity of the flow cytometer. This made it difficult to accurately analyse the samples and may partially explain the large variation in the results.

(Following page)

Figure 4.1 Experimental design of infection experiments. 5L culture grown to mid exponential phase of growth curve (approximately 5×10^5 cells ml⁻¹) was divided into four 1L cultures.

a In experiment one, culture A was the control with no viruses added, culture B was infected during the G1 phase at 0 h, culture C was infected during the S phase at 8 h, and culture D was infected during the G2 + M phase at 14 h.

b In experiment two, culture A was the control with no viruses added, culture B was infected during the G2 + M phase at 0 h, culture C was infected during the G1 phase at 10 h and culture D was infected during the S phase at 18 h.

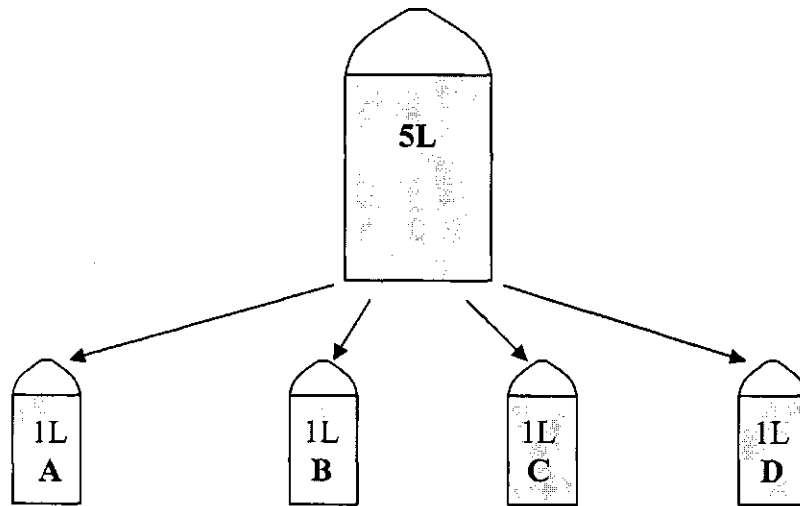
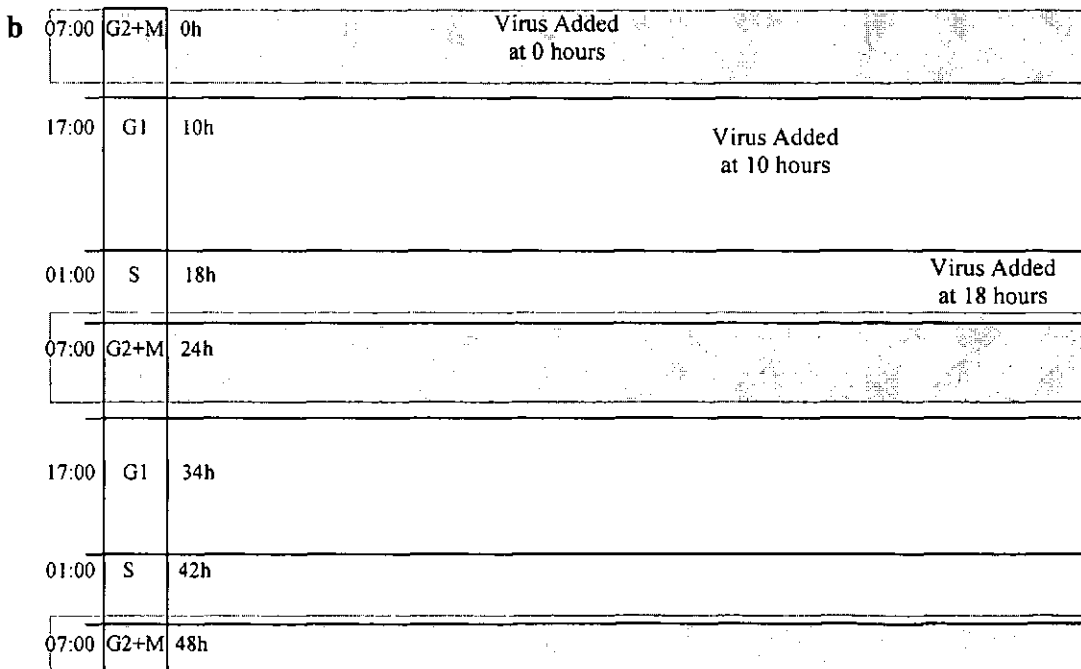
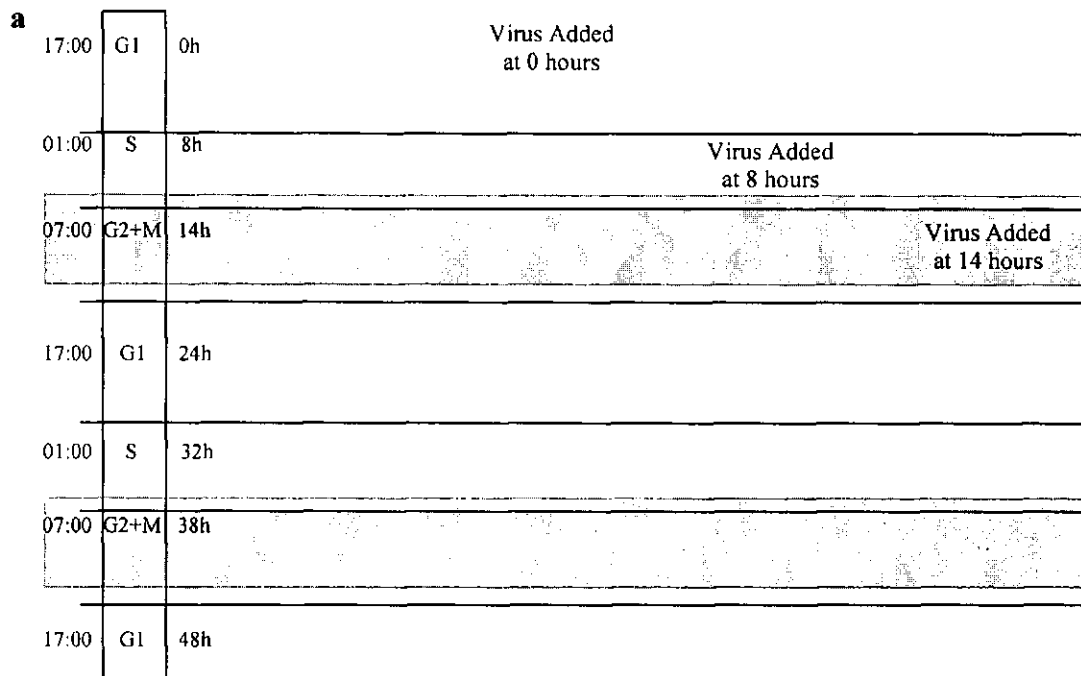


Figure 4.1



(Following pages)

Figure 4.2 Flow cytometry frequency histograms of green fluorescence showing cell cycle phase in all cultures at different times of the infection experiments. Infection experiment one (a) and infection experiment two (b). In a, the 38 h S phase sample is missing due to a sampling error. In b, the 0h control sample is missing due to an analysis error. Dark phase marked with grey boxes. Infection point of cultures marked with red box.

Figure 4.2a

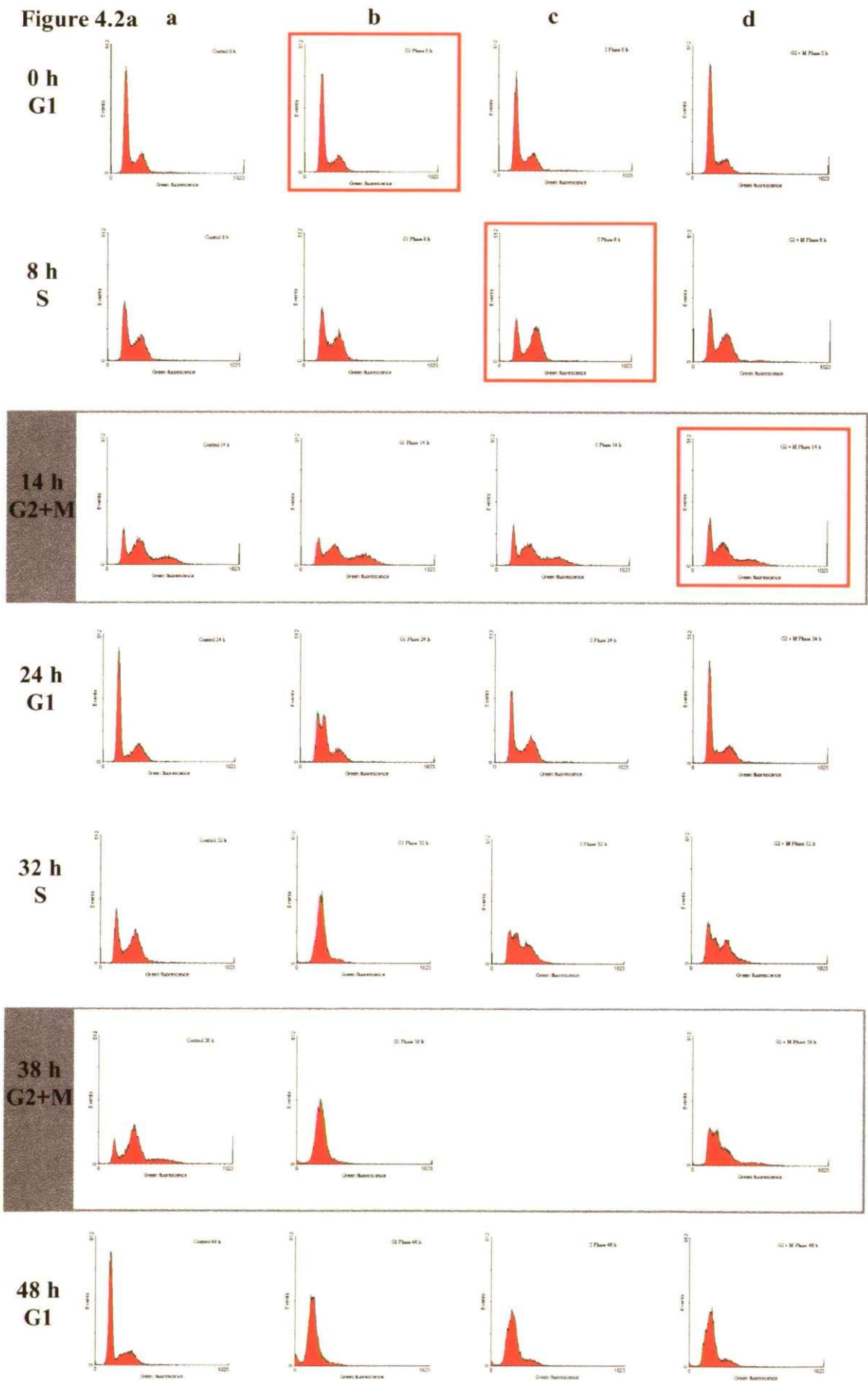


Figure 4.2b a

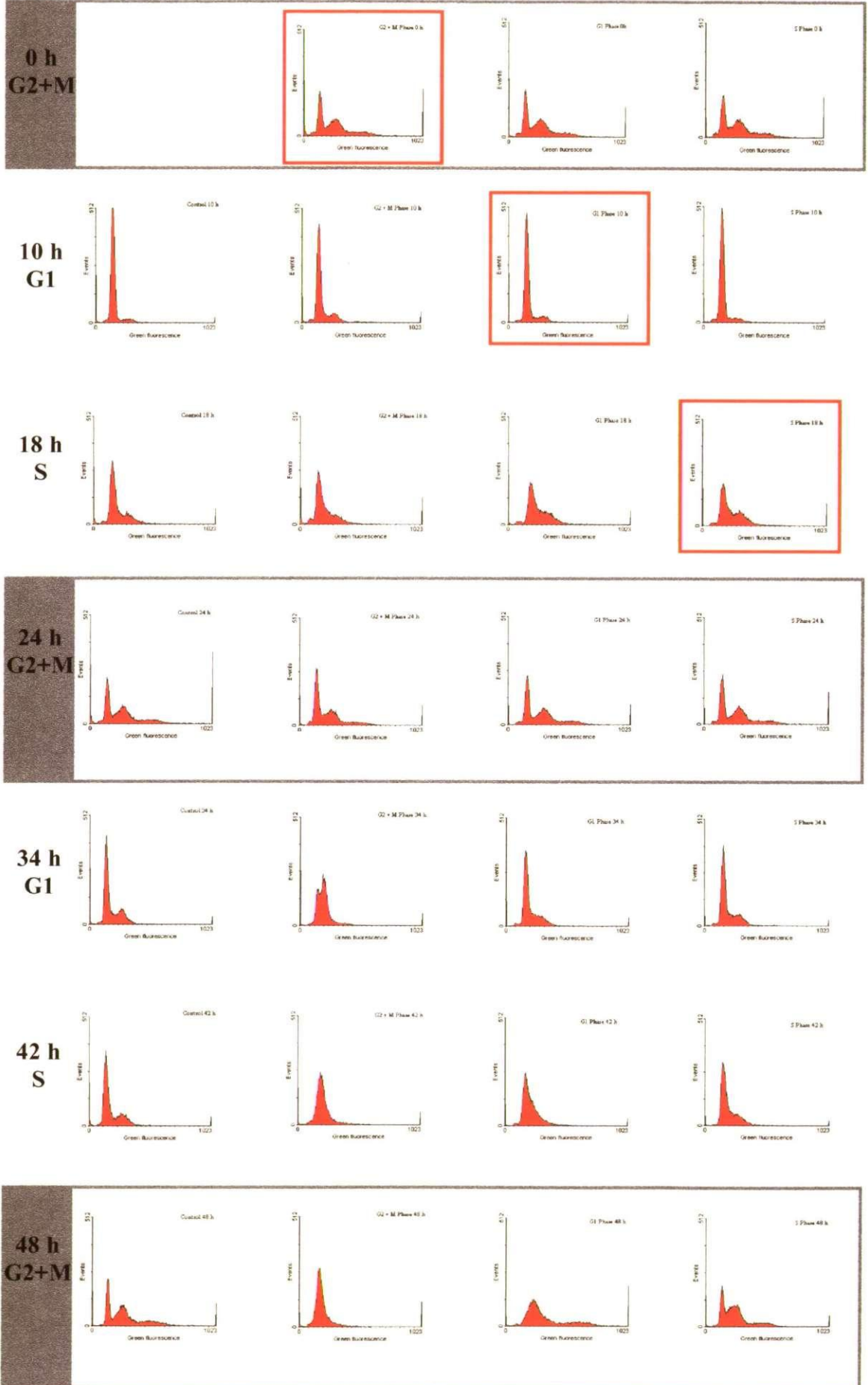


Figure 4.3 Changes in numbers of *E. huxleyi* in 2n and 4n populations during infection experiment two (populations shown in fig. 3.3). Control (a), G2 + M phase infected (b), G1 phase infected (c) and S phase infected (d). The samples for the control culture at the first two time points are missing due to analysis error.

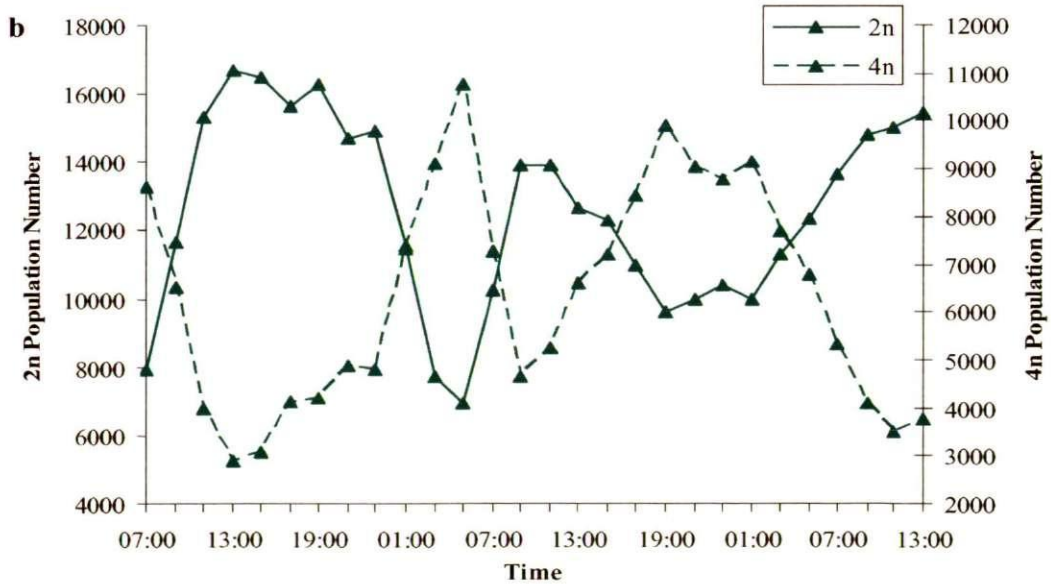
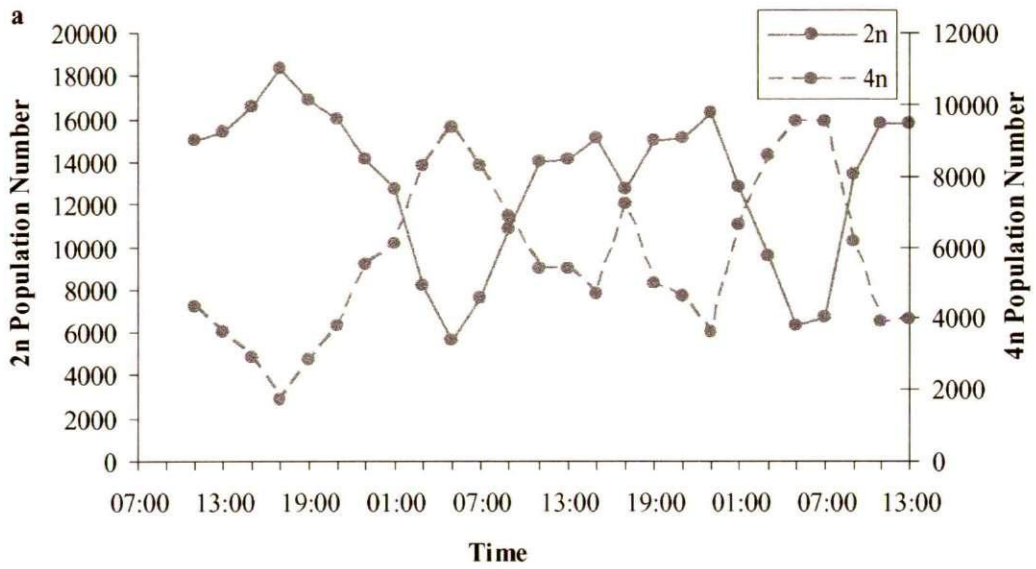
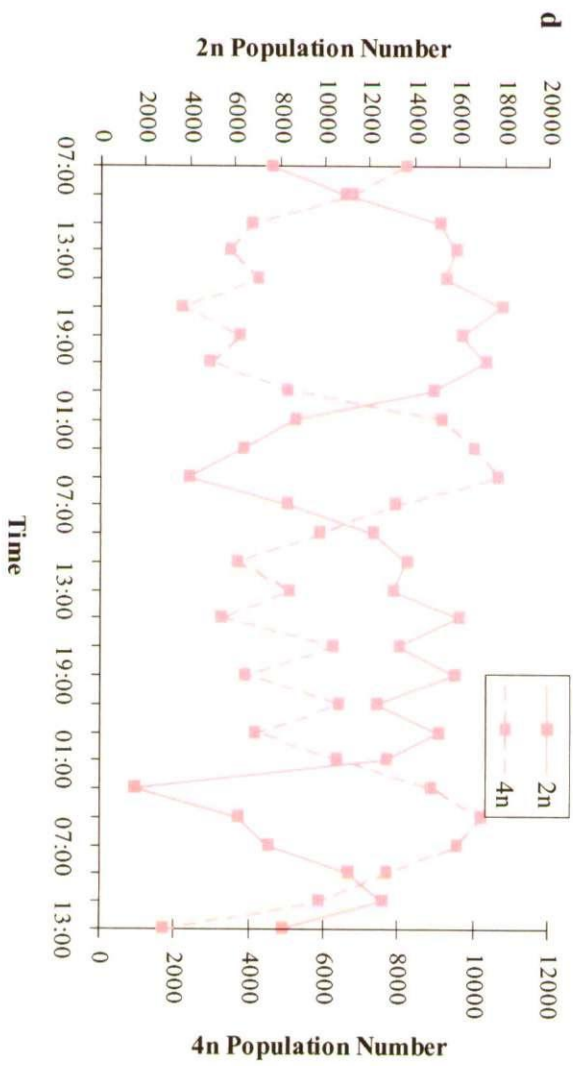
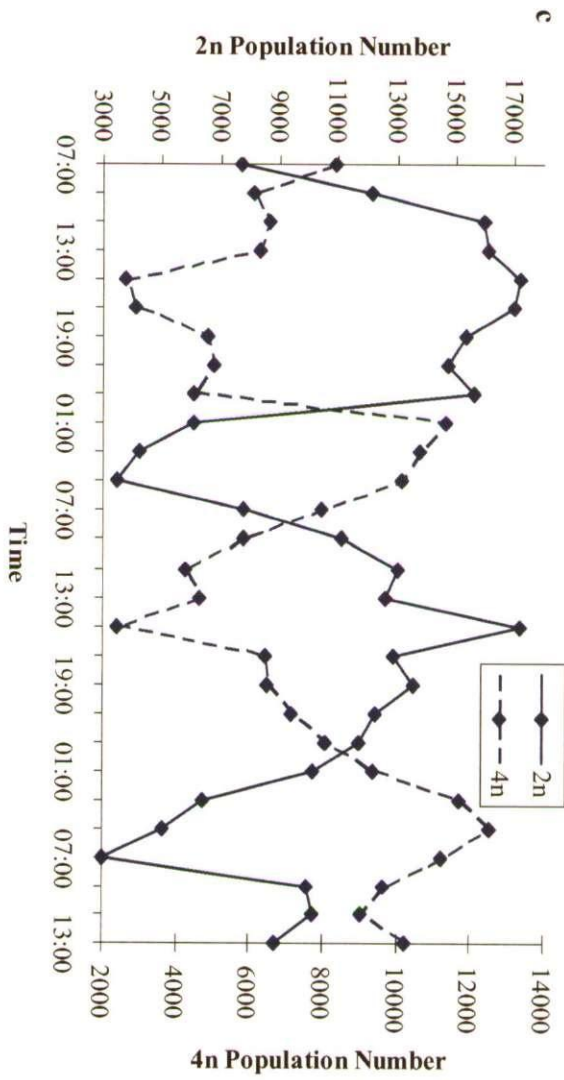


Figure 4.3 continued



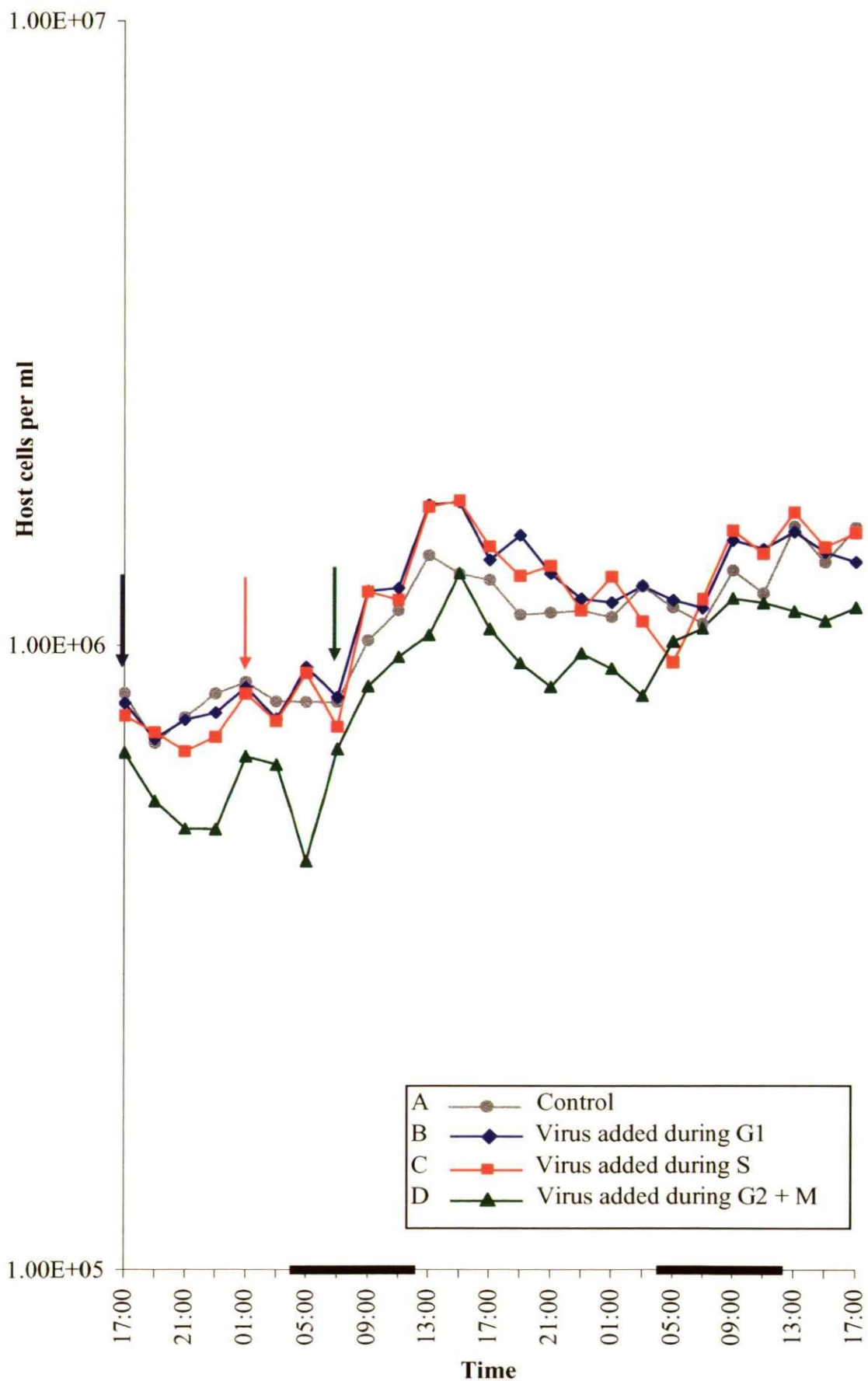


Figure 4.4a Host *E. huxleyi* numbers from infection experiment one (fig. 4.1a). Dark phases marked with black bars. Arrows indicate point of infection. Control grey, G1 phase infected blue, S phase infected red, G2 + M phase infected green.

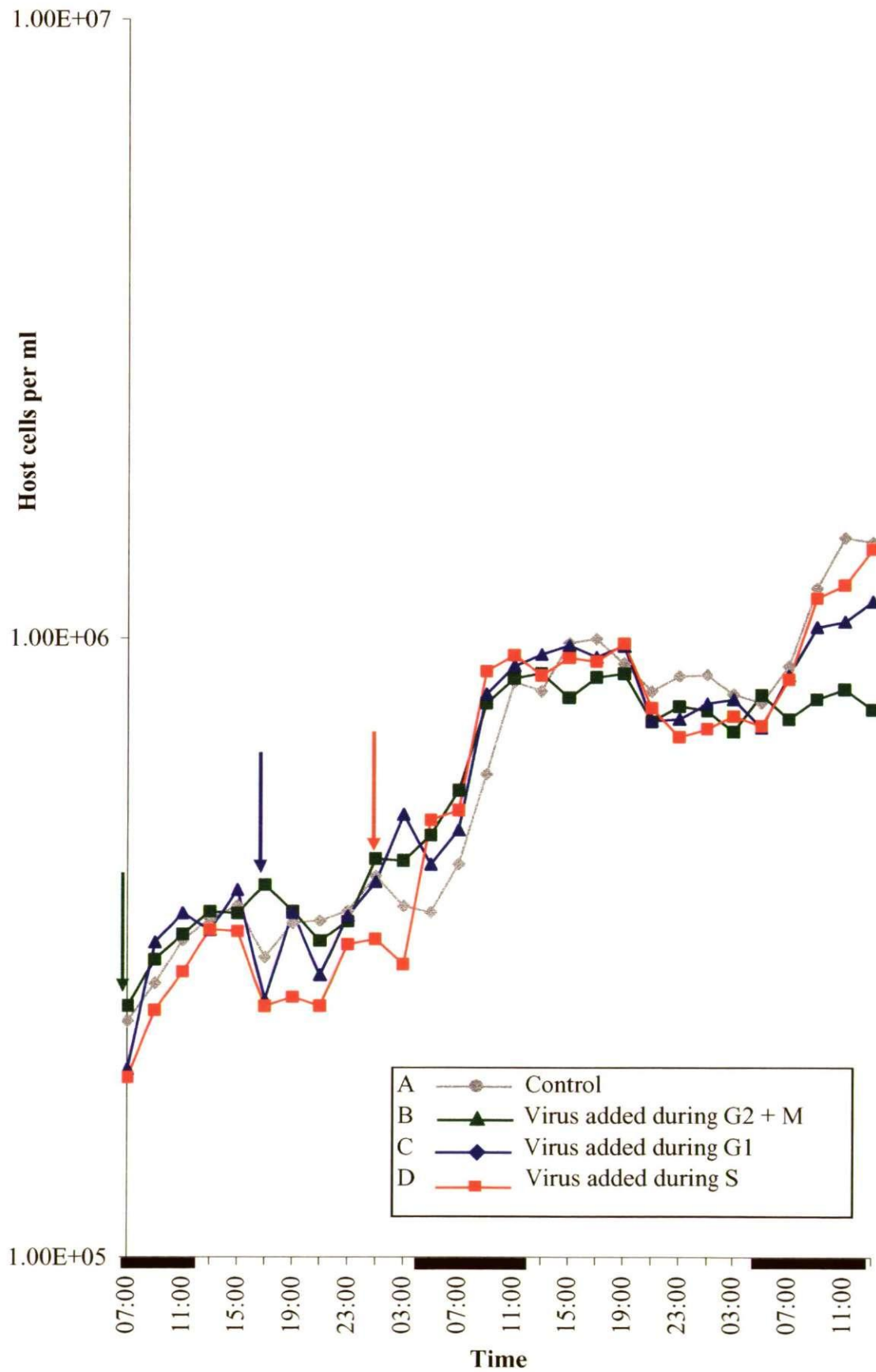


Figure 4.4b Host *E. huxleyi* numbers from infection experiment two (fig. 4.1b). Dark phases marked with black bars. Arrows indicate point of infection. Control grey, G2 + M phase infected green, G1 phase infected blue, S phase infected red.

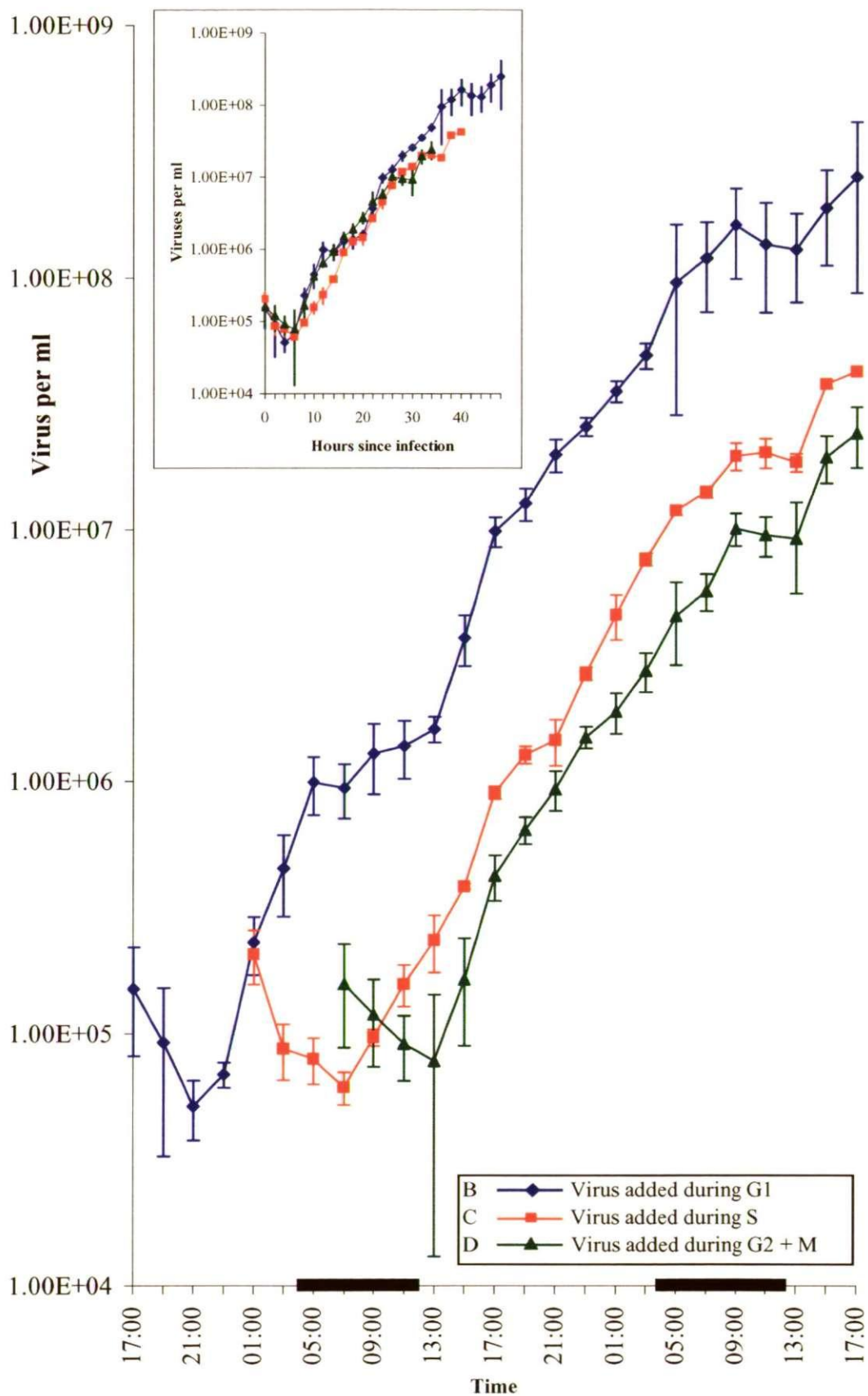


Figure 4.5a Virus numbers ± 1 SD in infection experiment one. Dark phases marked with black bars. G1 phase infected blue, S phase infected red and G2 + M infected green.

Inset virus numbers from time of infection.

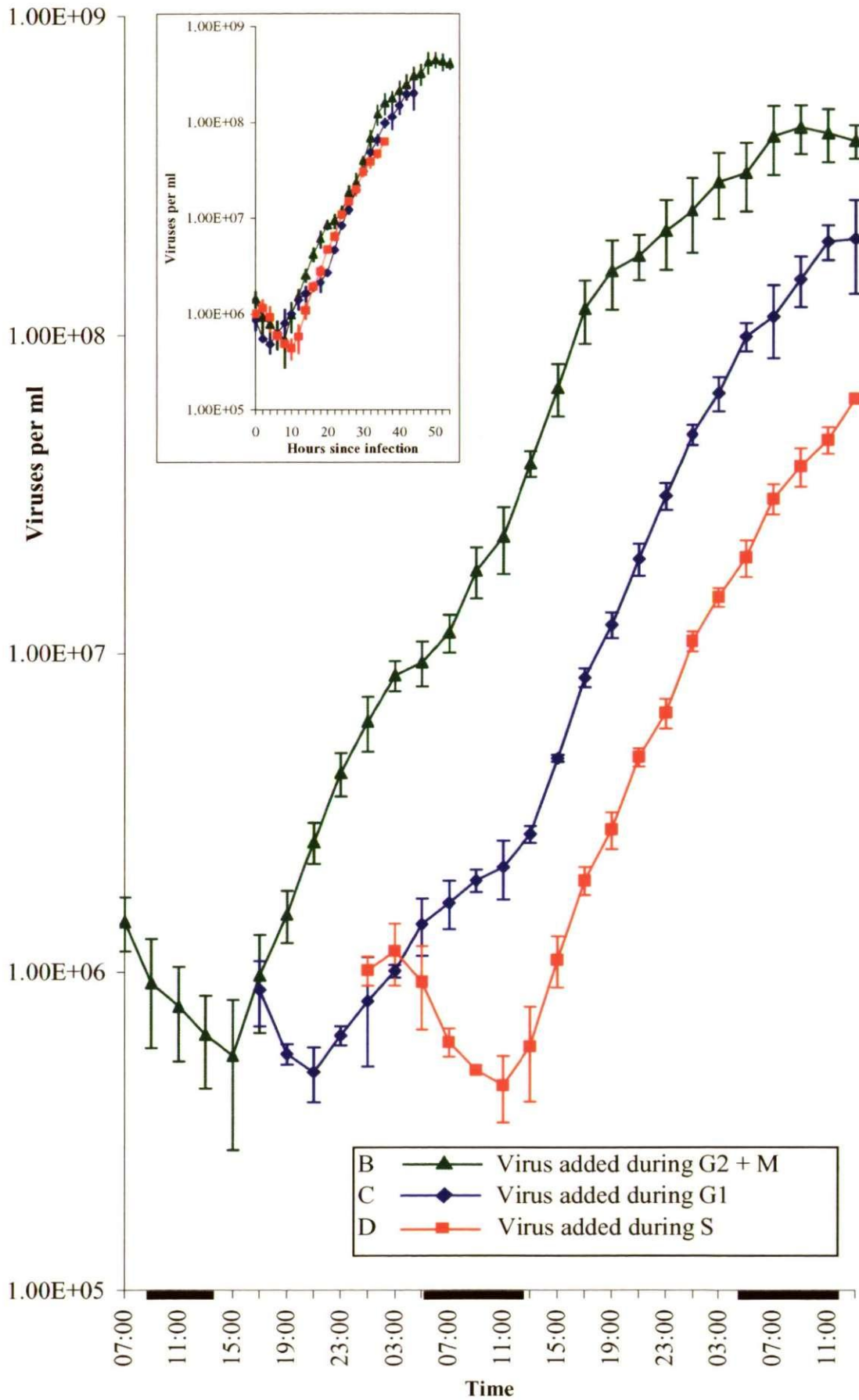


Figure 4.5b Virus numbers ± 1 SD in infection experiment two. Dark phases marked with black bars. G2 + M infected green, G1 phase infected blue and S phase infected red.
Inset virus numbers since time of infection

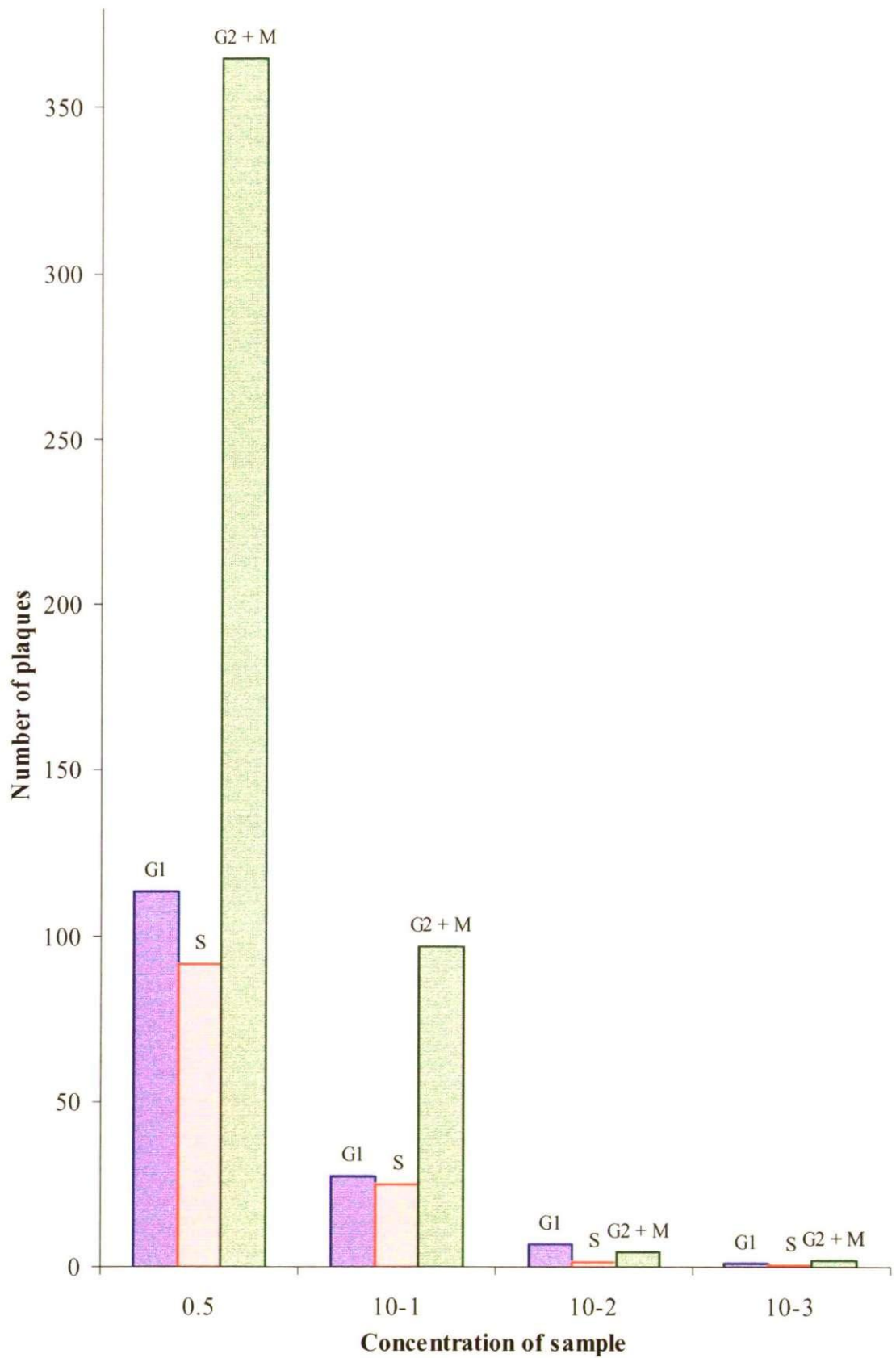


Figure 4.6 Numbers of plaques in plaque assays from each culture 2 hours after infection, at various concentrations.

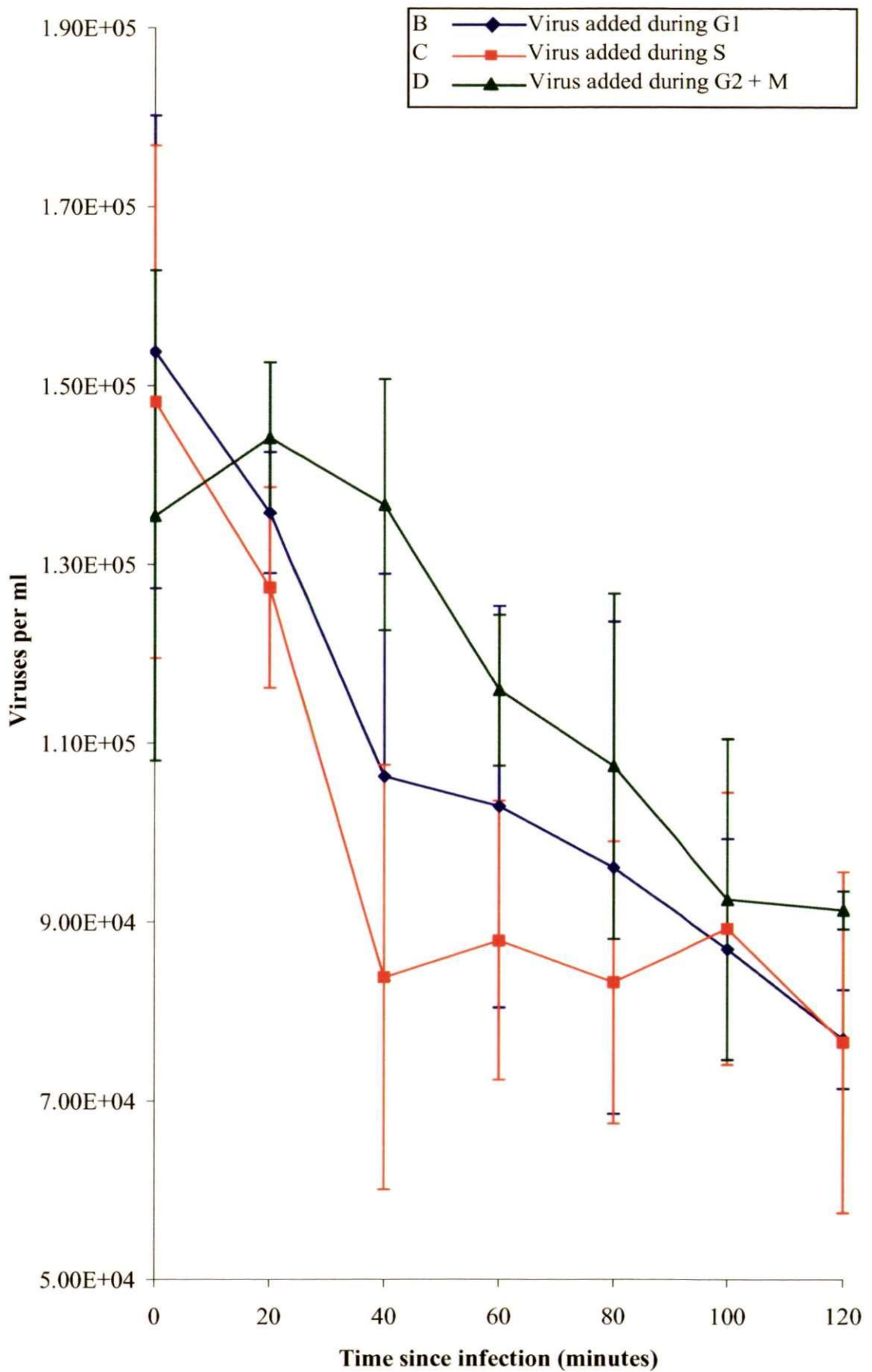


Figure 4.7a Numbers of viruses during the 2 hours following infection in each culture \pm 1 SD, during adsorption experiment one. G1 phase infected blue, S phase infected red, G2 + M phase infected green.

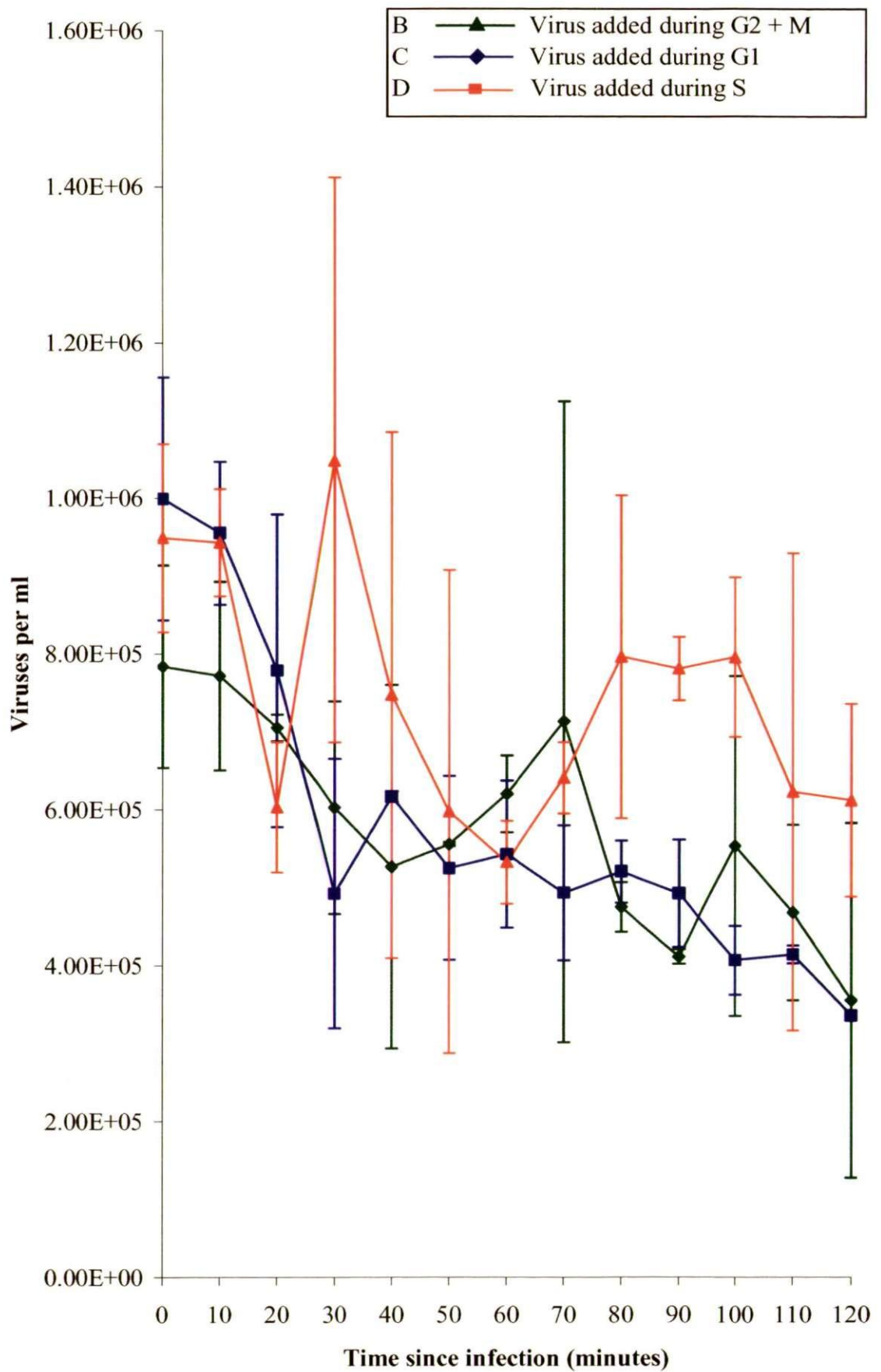


Figure 4.7b Numbers of viruses during the 2 hours following infection in each culture \pm 1 SD, during adsorption experiment two. G2 + M infected green, G1 phase infected blue, S phase infected red.

5. Additional Observations During Sample Analysis

During analysis of samples, many flow cytometry images were recorded. Each image provides a detailed log of a sample which can be used to compare different time points or experiments. During these experiments a number of changes within the samples were observed from the flow cytometry plots.

5.1. Live host

During both infection experiments, changes were recorded in the live host plots which showed a loss of the typical population signature (fig. 5.1). In the early stage of the experiment (fig. 5.1a), the host population closely matches the typical host plot (fig. 2.2). As the experiments continue, the host population gradually increases in size on both axes until reaching a large and more dispersed population than during the earlier stages of the experiment (fig. 5.1b). The population has wider range of red fluorescence and side scatter, and overall it is less densely clustered than in the early stages of the experiment. These changes could be due to the viral attack and the subsequent damage they have on the host cells. Damage to the internal components of the cell and the presence of viruses will alter the red fluorescence reading, the lysis of the host cells will result in oddly shaped and sized cell fragments which will register as a wider range of side scatter.

These observations are similar to changes found by Jacquet *et al.* (2002) during the collapse of an *E. huxleyi* bloom due to viral activity. They recorded an extra population occurring as free virus numbers increase; the extra population had a lower right angle light scatter but the same red fluorescence as the early *E. huxleyi* population. They attributed this to a new form of *E. huxleyi* with few or no coccoliths (the population was lithed at the beginning of the experiment). The typical reduction in chlorophyll *a* fluorescence which would signify lysed cells was not recorded by Jacquet

et al. (2002), (however from their flow cytometry plots (fig. 2) it is possible to see that there is a small population which display this characteristic decline). It was suggested that the change to the non-lithed population may be linked in some way to virus activity.

Comparing the results seen in this experiment with those of Jacquet *et al.* (2002) it is possible that this population may be showing both changes to a non-lithed population, but that there also appears to be the remains of lysed cells. This accounts for the changes in red fluorescence and side scatter.

5.2. Virus Population

The virus numbers during the experiments range from the lowest detection thresholds of the flow cytometer during the first hours after infection, up to samples which exceed the 1000 events per second upper threshold and require further dilution in order to gain an accurate result.

Changes become apparent in the virus population over time, in both infection experiments (fig. 5.2). This took the form of additional virus populations appearing. In infection experiment one there are two extra populations, one with higher green fluorescence and lower side scatter, the other with higher green fluorescence and side scatter which appears like a comet with a dense population and a tail of reducing virus density. In the second infection experiment a third extra population is visible in addition to the two seen during the first experiment, having the same green fluorescence but higher side scatter. The original virus population remains present in all samples of both experiments. These changes could be due to the large number of viruses clumping together, which would explain the populations with higher green fluorescence as the flow cytometer would record a clump of viruses as one particle with the combined green fluorescence of a number of viruses. As virus numbers increase, there is more chance

of viruses with variations in structure being present which would account for changes in the side scatter range.

In all the virus sample analyses, it was necessary to increase the dilution of the samples as the virus numbers increased to maintain accurate recordings. Flow cytometry samples have to be 1ml to allow for calculations of virus numbers, so when increasing the virus dilution the virus sample volume is reduced and the TE volume is increased (section 2.2.1.1.). During the second infection experiment, it was noticed that this caused a change in the green fluorescence level of the population; more dilute samples had a higher green fluorescence reading (fig. 5.3). This suggested that the TE affected the staining process of the viruses and thus influenced the green fluorescence of the cells.

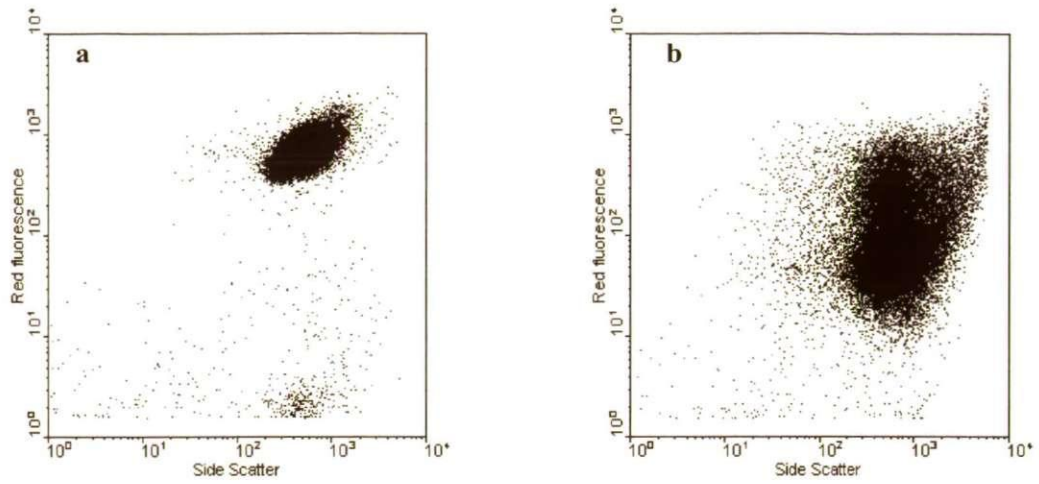


Figure 5.1 Scatter plots of *Emiliana huxleyi* populations at the 6 hour time point (a) and at the 102 hour time point (b) of the infection experiment. The changes in the range of red fluorescence and side scatter suggest the deterioration of the cells during increased virus exposure.

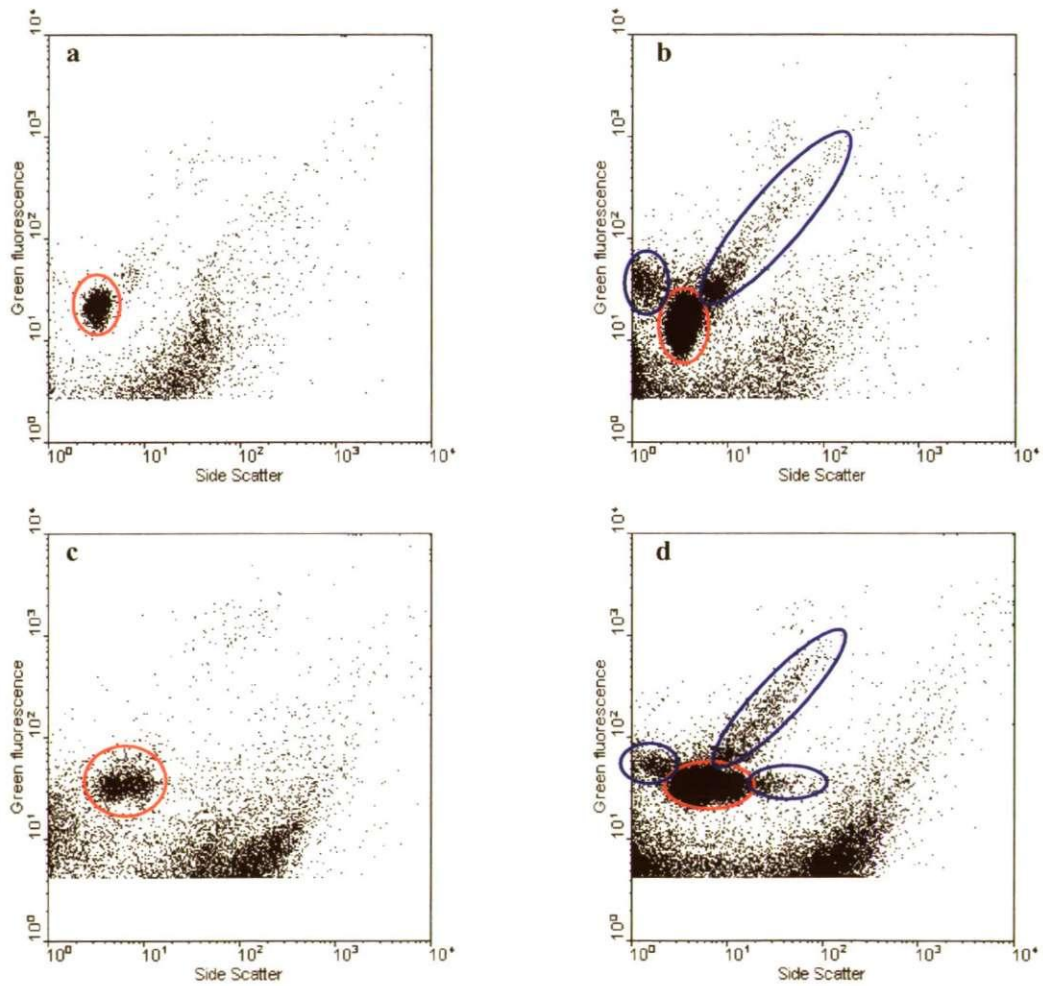


Figure 5.2 Scatter plots of virus groups early and late in the experiment: infection experiment one: early virus group (20 hours) (a) late virus group (74 hours) (b) and infection experiment two: early virus group (26 hours) (c) late virus groups (78 hours) (d). 'Typical' virus population is circled in red, additional virus groups are circled in blue.

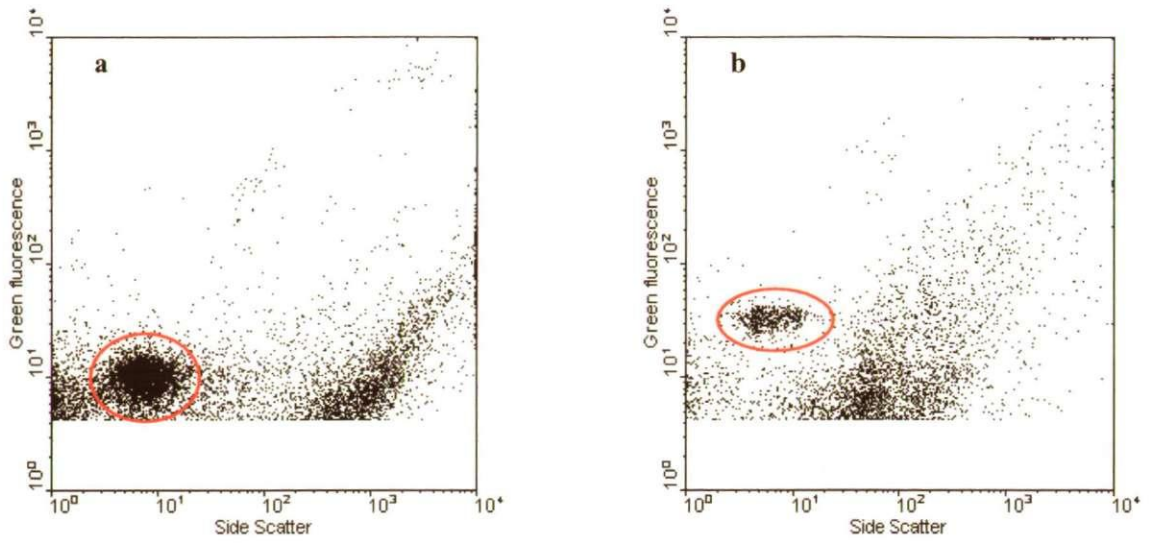


Figure 5.3 Virus groups at the 22 hour time point during infection experiment two. Plots demonstrate the increase in green fluorescence following greater dilution of samples. 1:10 sample (**a**) and 1:100 sample (**b**).
Virus population circled in red.

6. Discussion

The aim of this research was to investigate the host:virus relationship in an ecologically important marine phytoplankton, *E. huxleyi*, with an emphasis on how host cell cycle phase may influence infection. This has been accomplished through a series of experiments centring on: virus adsorption, infection and production and host lysis and cell cycle. In this chapter I shall discuss the results found and in the next chapter endeavour to answer the questions which formed the initial aims of this project and provide the overall conclusions of this work.

6.1. Infection Experiment One (IE1)

In this experiment, three *E. huxleyi* cultures (1l) were infected with EhV86, one at each of the following phases: G1 phase (17:00 h), S phase (01:00 h) and G2 + M phase (07:00 h) (fig. 4.1a). The aim was to test the hypothesis that virus production was host cell cycle dependent: if this was the case, one phase would have a greater amount or rate of virus release. If the null hypothesis was supported then all cultures would have a similar amount and rate of virus release.

All infected cultures crashed four days after virus was added showing that all phases of host cell cycle are vulnerable to virus attack. Virus release was at a similar rate and quantity in all cultures (fig. 4.5a). This supported the null hypothesis that virus production is host cell cycle independent.

If virus production is cell cycle independent, this suggests that infection causes a series of events which take a particular length of time to complete; this would lead to all effects of infection occurring over the same period of time following infection, regardless of infection phase. This would lead to collapse of the host culture the same number of hours after infection in each culture. This is not the case (fig. 4.4a, table 4.2). In this experiment, all cultures crashed at the same time despite there being a

delay in the infection times: the S phase was infected 8 hours after the G1 phase and the G2 + M phase was infected 14 hours after the G1 phase. If virus production is cell cycle independent, then the G1 culture would collapse first, followed by the S culture 8 hours later and the G2 + M culture a further 6 hours later. This result conflicts with the conclusions drawn from the virus release numbers. There is no difference in the virus production but the faster lysis of the G2 + M culture suggests that there is a greater efficiency of viruses infecting during this phase and therefore this is a cell cycle dependent result.

This experiment found that cultures infected during the G2 + M phase lysed faster than cultures infected in the G1 or S phase. Based on this result, it is predicted that if the infection experiment begins with the G2 + M phase infection (followed by the G1 and S phase infections), the G2 + M culture will crash a day earlier.

6.2. Infection Experiment Two (IE2)

This experiment tested the prediction from IE1 by altering the order of infection of the *E. huxleyi* cultures (fig. 4.1b).

The results again showed virus release to be the same in all cultures (fig. 4.5b) with the exception that the G2 + M virus numbers begin to plateau quite clearly with a narrow margin of variation, whilst the G1 and S cultures are still increasing. This contrasts with the slight plateau which occurs in the G1 phase in IE1 where there is a large amount of variation.

The host number results support the prediction that the G2 + M culture would lyse one day before the G1 and S phase cultures. However, the initial signs of culture collapse in IE2 occur later than in IE1 (table 4.2). Collapse begins 18 hours later in the G2 + M phase (48 hours after infection compared to 30), but only 4 hours later in G1 and S phases (52 and 60 hours after infection respectively). It can be seen in figure 4.4b

that the G2 + M culture does not complete the third cell division whereas the G1 and S phase cultures do. (In IE1, it appears that the G2 + M culture does not complete the second division but this is actually due to the host numbers in the G2 + M culture being slightly lower than the other cultures throughout the whole experiment.) All cultures in IE2 have similar host numbers and the G2 + M phase is beginning to collapse when it fails to divide. After this the G2 + M host cell numbers decrease but the other cultures remain in healthy numbers after completing a full division.

This comparison of patterns within the datasets needs to be considered in the light of some key differences between the experiments. The first difference is the stage of the growth curve the host cells are in. Host cell numbers during IE1 are higher signifying that they are further up the exponential stage of the growth curve. This is supported by the smaller increase in host numbers after each division phase compared to the larger steps up in the second experiment host numbers: the culture in IE1 is one day further into its growth curve. This has important implications for virus activity as the larger step increases at each division phase in IE2 produce more new host cells into the culture than the division phase in IE1. This is acting as counterbalance for the host cells lost through viral attack and explains why the cultures take longer to collapse in IE2 (table 4.2). Greater production of hosts during infection of the culture is enabling the population to resist the total crash for longer (table 4.2). Despite the onset of collapse being delayed by only 4 hours in the G1 and S cultures, their complete collapse was delayed by a day; conversely, in the G2 + M culture, collapse began 18 hours later, but total collapse still occurred on the fourth day of the experiment. This again shows that virus attack during the G2 + M culture is more virulent.

From the results discussed so far, it is clear that there is some aspect of infection during G2 + M phase, whether it is due to the host, virus or the environment, that makes this phase most efficient phase in terms of virus activity. Thyraug *et al.* (2002) found

that cultures of *P. orientalis* infected when the culture had previously been in dark conditions (at the end of the dark phase or the beginning of the light phase) produced a greater number of viruses than if it was infected after being in light conditions. This also supports the findings here that the G2 + M phase is the most efficient phase for virus infection.

The G2 + M phase is the only phase of infection which occurs during the dark and it is the phase of mitosis and cell division. We should bear this in mind as we examine the other aspects of host:virus activity observed during these experiments and try to ascertain whether there are any further differences between the G2 + M phase and the G1 and S phases.

6.3. Cell Cycle

The cell cycle samples taken during the infection experiments have provided an interesting insight into how the host activity changes following infection. In both experiments, the host cell cycle was well synchronised and all cultures exhibited the same phases as the control culture during the first 24 hours of the experiment (fig. 4.2 and 4.3). After this point, changes began to occur in the host cell cycle activity (table 4.1). There was a gradual deviation from the activity seen in the control culture as the infected cultures moved towards a single peak, with a wide base and a peak green fluorescence slightly above G1 of a 2n population.

This state does not match to any of the cell cycle phases, so the activity of the host is unknown. As the peak appears, in most cultures, split peak is visible. It is possible that this is a distinction between the uninfected host cells (providing a lower mean green fluorescence) with a peak of infected host cells present (providing a higher green fluorescence signal due to the DNA content of the viruses within the cell).

6.3.1. Cell Cycle Tests

There is an anomaly within the sets of cell cycle data collected during this project. The second cell cycle test revealed a very obscure set of histograms (fig. 3.2). It was possible to establish the required cell cycle data from the scatter plots collected despite this. However, when the second infection experiment was run two weeks later, the cell cycle histograms were acceptable to identify the cell cycle with (fig. 3.2 and fig. 4.2b) and showed a population with a synchronised cell cycle. When compared to the cell cycle data collected in the first infection experiment, it is possible to see that the host culture also appears to be better synchronised in the later experiment, therefore suggesting the multi-ploidy populations are not as prolific as they had been.

This could show that the cultures were still adjusting to their new light:dark cycle when the tests were done, and that more frequent culturing was also benefiting the synchronicity of the culture.

6.4. Adsorption and Infection

Adsorption of viruses was specifically recorded on two occasions by counting the free viruses in each infected culture for the two hours following infection. This was done every twenty minutes in the first experiment and every ten minutes in the second experiment. Plaque assays were run parallel to the virus samples to measure infection success. Unfortunately the plaque assays performed in the second experiment yielded no results. This has led to the lack of an important data set which would have been especially interesting in light of the differences between the two infection experiments. However, the data that was successfully collected has proved to be a key part of this experiment.

It was hypothesised that if there was a cell cycle dependent result in the infection experiments, there would be a correlating difference in the adsorption and infection of

viruses: it is logical to assume that if a virus has greater efficiency from infecting during a particular phase, then greater adsorption and infection will also occur. It may even be that the higher rate of adsorption and infection may be responsible for the differences seen.

The virus data from these two experiments (fig. 4.7) showed no significant difference in the adsorption rate of viruses due to the very large variation in the data. These samples contain virus numbers which are at the lowest detection threshold of the flow cytometer and this is thought to have made this analysis less accurate. For example, a number of the S phase samples in the second experiment (fig. 4.7b) were particularly noisy, as they contained particles which were recorded in a large region which encompassed the virus population. This led to higher virus numbers being recorded and is a partial explanation of the obscure result seen in this dataset.

The successful plaque assays from the first experiment revealed an important aspect of this system (fig. 4.6): the G2 + M phase had three times more successful infections than the G1 or S phase cultures. Combined with the virus release data from IE1 and IE2 which shows the largest virus release during the light phase (fig. 4.5), this contradicts the usual understanding of virus release and infection. Because viruses are vulnerable to damage by UVR, it is predicted that there will be greater adsorption and infection during the light phase so that viruses are protected from damage by their hosts. Virus release is predicted to occur mainly during the dark phase when they are not at risk to UVR. Jacquet *et al.* (2002) recorded this pattern in virus release during an enclosure experiment of an *E. huxleyi* bloom. The results presented here contradict that finding, as the largest numbers of viruses are released during the light hours and the greatest infection occurs in the dark. This suggests that the releases of viruses at high host densities are enough that, had they been in a UVR system, then the losses through UVR damage would have been minimal compared to the net gain of virus progeny.

Viruses are adsorbed at a similar rate during all phases (fig. 4.5 and 4.7) but there is a difference in infection success between the phases (fig. 4.6), this suggests two things: 1) the host may be more vulnerable to infection during this phase or 2) the viruses may be more virulent during this phase. In the G1 and S phases, viruses are reaching the surface of the host but not being as successful at entering the cell. It is possible that the host cells being infected during the G1 and S phases are actually G2 + M phase cells but they are out of sync with the rest of the population. Figure 4.2 shows that there are some cells which are in the 'wrong' phase, although this may be the presence of the multi ploidy groups so is therefore not a conclusive answer.

The division of host cells during the G2 + M phase could be a key point of this relationship. The viruses require the host so that they are able to reproduce, which leads to the suggestion that maybe this is the best phase for infection because viruses are able to replicate immediately. This could be enabled by the virus responding to changes in the cell surface proteins, acting as signals of the cell changes. The converse of this is that the viruses are able to control the host once they have infected so they would have no need to wait for signals of the G2 + M phase.

Physical changes may occur in the host at the point of cell division which may facilitate greater levels of infection. If there is a reduction in the covering of coccoliths as the daughter cells divide it could lead to the cell surface being more vulnerable to infection. This is supported by data which shows greater infection rates in naked strains of *E. huxleyi* (van Bleijswijk *et al.*, 1996), however this evidence is contradicted by Schroeder *et al.* (2002) who found the naked and scaly strains of *E. huxleyi* to be resistant to infection. However, the CCMP 1516 strain of *E. huxleyi* used here is vulnerable to infection in its lithed form, so therefore it is also likely to be vulnerable to infection when it may have a reduced covering of coccoliths, which may occur during or following division.

6.5. Virus Release

There is a general pattern of virus release seen in all infected cultures (fig. 4.5). The pattern consists of an adsorption phase where the viruses are lost as they attach to hosts. After this point the virus numbers increase at a near constant rate until reaching a plateau on the fourth or fifth day which corresponds with the collapse of the host cultures (data not shown). Within this pattern, there are three main points of variation

The first variation is between the experiments, the virus numbers during IE1 are an order of magnitude lower than in IE2. This was an unintentional experimental difference, and it may be predicted that more viruses at the start would result in a greater net gain of viruses during the experiment. This is not the case as IE2 has approximately half a magnitude less viruses at the end of IE2, although this is a statistically insignificant difference as the variation in the samples overlaps. Thyrraug *et al.* (2002) infected their cultures with different host:virus ratios varying by an order of magnitude to investigate how this would effect virus production in a slow infecting microalgae *P. orientalis*. They found that the virus release numbers were correspondingly higher in the higher host:virus ratio cultures. Because this trend was not observed in this experiment, it suggests that at the lower virus numbers the optimum host:virus ratio was present, and any increase in the number of viruses would not lead to a greater virus production.

The next variation in the virus release occurs in the length of time viruses are adsorbed for. Adsorption is the attachment of viruses to a surface, it is assumed that virus loss through attachment to non-host surfaces will be at the same proportion in all the cultures, therefore the differences between adsorption times and virus numbers is as a result of difference to host attachment. Adsorption to a host does not necessitate infection and is also reversible: viruses can un-attach from a host if unfavourable conditions are encountered. Adsorption is visible as a drop in numbers occurring in all

cultures after infection and lasts for 4 to 10 hours. In both experiments, adsorption during the G1 phase only occurs for 4 hours, whereas it occurs for 6 hours in G2 + M and S phases in the first experiment and 8 and 10 hours respectively in the second experiment. In comparison to the adsorption during the infection experiments by Thyrrhaug *et al.* (2002), the adsorption in the *E. huxleyi* cultures appears to be quite dramatic and rapid. In the Thyrrhaug *et al.* (2002) cultures, there is a latent period of 18-20 hours after infection and during this time, the drop in virus numbers is small compared to the drop seen in this species. This shows that the *E. huxleyi* infection processes works quicker than in *P. orientalis* and adsorption of viruses is more dramatic than in *P. pouchetii*, which may have implications for the bloom activity of this species.

As discussed in section 6.4, there is greater infection of viruses during the G2 + M phase. This explains the final point of variation in the virus release pattern. Following adsorption, the virus number increases at steady and high rate except for during the dark phase when a plateau of virus release occurs. There is a clear reduction in virus release during the dark phases in infection experiment one (fig. 4.5a) and a slightly less clear in the second experiment (fig.4.5b) although there is overlap of the error bars during the dark phase which only occurs rarely during the light phase, therefore showing a distinct slowing of virus increase. When considering both sets of data together, it appears that the plateau effect is due to an increase in virus infection, which would reduce the number of viruses which had adsorbed and may un-attach following unsuccessful infection.

6.5.1. Confounding

The aim of this experiment was to observe how virus production varied when host cultures were performing different functions at the point of infection. The nature of this system hinders this. From the results, it is possible to see a general pattern: viruses are

lost from the free water, and assumed to be adsorbing to host cells. After 4 – 10 hours of adsorption, hosts that were first infected begin to lyse, releasing a fresh supply of viruses into the water. These viruses will then adsorb to the hosts which were not infected by the first viruses, but by this time the hosts have moved into a different phase, so the culture no longer contains host cells only infected in a specific phase. From figure 4.5, it is evident that there is a near-continual release of viruses and therefore, it is likely that there is a constant infection. The number of viruses being released during the experiment is also much greater than the number added at the beginning of the experiment: figure 4.5 shows the numbers of viruses per ml. The experiment is started with the addition of 2ml of virus lysate, but the difference between each sample taken is multiplied by over 800 times to account for the volume of the culture (at each time point, 7.5ml of culture is removed; the culture starts at 1l reduces to approximately 800ml by the 48 hour time point).

This apparent negative aspect of the experiment may help to understand some of the data, which initially does not appear to match the conclusions of other datasets from the same experiment. If the hosts are being exposed to a continual bombardment of viruses, then it is probable that the virus release in each culture will be similar as they are all actually experiencing the same conditions. There would only be a difference in virus number, if there was only one phase when the viruses could successfully infect the cells. Figure 4.6 illustrates clearly that some infection can occur during all phases therefore discounting this possibility.

In the infection experiment of *P. orientalis* and *P. pouchetii*, Thyshaug *et al.* (2002) find a difference in virus production dependent upon phase of infection only in *P. orientalis*. In *P. orientalis* there is a, 18-20 hour lag between the infection point and the beginning of virus release. This release is therefore a direct result of infection during a specific phase and is a more accurate test of the effects of host cell cycle on virus

production. The infection of *P. pouchetii* was not cell cycle dependent, but the adsorption phase is shorter and shows greater virus loss from the suspension, so therefore virus release further infections may be occurring before an accurate cell cycle phase specific result is acquired.

The scenario in the *E. huxleyi* host:virus systems appears that despite the inability to clearly identify if virus release is variable with cell cycle, there are still cell cycle dependent trends being observed. If a host is infected during the G2 + M phase, it is immediately exposed to a higher rate of infection. This, in effect gives the viruses in a head-start at collapsing this culture compared to the infections beginning in the G1 and S phases as these will experience lower rates of infection success for a number of hours, until the host reaches the G2 + M phase, by which time the G2 + M infected culture will be undergoing another higher rate of infectivity. This provides a clear understanding as to why this culture crashes so quickly in the infection experiments (fig. 4.3 and 4.4).

With this final point about the continuous infection of the cultures, it is possible to explain why the 3 fold increase in infection during the G2 + M phase does not result in a 3 fold increase in virus release, 6 hours after the G2 + M phase. It could be that the continuous lysis and infection occurring acts to smooth out any differences which may be happening. It may also be a result of numbers: during G2 + M, all the 'available' hosts may be infected within 40 minutes of virus addition, and in the G1 and S phases, it takes 120 minutes to infect the same number of hosts. Therefore, if this resulted in a variation in the virus release rate, it would not be recorded at this level of sampling.

From looking at the graphs of the virus release data (fig. 4.5) it is difficult to accurately analyse if there are and differences in the rate of virus release, out side of the clear dark phase plateau. To scrutinize this aspect of the data, the slopes of the virus release plot could be recorded and compared to see if there is an increased rate of release following the larger infectivity during the G2 + M phase.

7. Conclusions

This research set out to investigate the effects of *E. huxleyi* cell cycle on infection success, virus production and adsorption rate of viruses and host cell cycle during infection.

- The host was vulnerable to infection in all phases of the cell cycle. The infection success varied with a three times greater infection rate during the G2 + M phase of the host cell cycle. This was suspected to be linked to the division of the host cells occurring during this phase causing a change in the cell which facilitated easier infection, however this was not tested.
- Due to continual release and infection of viruses during the experiment, no clear pattern of cell cycle dependent virus release was observed.
- The adsorption rate of the cultures infected at each of the phases was not significantly different. The samples were difficult to gain accurate results from due to the virus numbers being at the lowest sensitivity of the flow cytometer which may have masked any differences between the cultures by producing large variation in the results.
- Cell cycle was synchronised in the cultures at the beginning of the experiments but infection caused the host cells to be compromised and remain in a fixed, unidentifiable stage of the cell cycle. This stage appeared to be similar to a G1 phase, but has higher mean green fluorescence and a wider range than would be predicted under non-infected conditions.
- It was also recorded that the stage of the host culture within its growth curve affected the length of time the culture took to crash. Younger host cultures took longer to crash due to the larger production of new host cells to counterbalance the loss of cells to virus attack.

The experiments carried out in this project have concentrated on small volume cultures at greater concentrations than *E. huxleyi* would be found in, in its natural environment. The work has revealed some interesting results that question previous beliefs about virus release during the day and virus adsorption being greatest at night. Younger cultures are also able to withstand mass mortality for longer periods of time, unless infected during the G2 + M phase.

The variation in infection rate may act as a protection mechanism to the host population as it prevents the most efficient rate of culture collapse occurring at all times. It is important that natural populations contain variation such as this as it allows both host and virus to perpetuate in the environment and maintain their roles within the plankton ecosystems.

8. Suggestions for Further Work

The results from this project have produced a number of further areas of study and new questions about this system. Further work on this aspect of *E. huxleyi* host:virus interactions could be orientated around these questions and further develop these ideas.

- The adsorption experiments could be repeated using a competitive attachment method whereby adsorption rate of viruses can be analysed to different method of recording the changing number of viruses.
- Observations of changes in the physiology of the host during the G2 + M phase through imaging such as electron microscopy.
- Fluorescent In Situ Hybridisation of the cell cycle samples would allow the presence of viruses within host cells to be recorded and may aid in the further analysis of the single cell cycle peak.
- The role of virus infection in *E. huxleyi* and what impacts this may have on the interactions of the host with other components of the natural system, such as grazers.

9. References

- Andreae, M. O. (1990). Ocean-Atmosphere Interactions in the Global Biogeochemical Sulfur Cycle. *Marine Chemistry*, **30** (1-3), 1-29.
- Bates, T. S., Lamb, B. K., Guenther, A., Dignon, J. and Stobier, R.E. 1992. Sulfur Emissions to the Atmosphere from Natural Sources. *Journal of Atmospheric Chemistry* **14** (1-4), 315-337.
- Bergh, O., Borsheim, K. Y., Bratbak, G. and Heldal, M. 1989. High Abundance of Viruses Found in Aquatic Environments. *Nature* **340** (6233), 467-468.
- Billiard, C. 1994. Life Cycles. *Systematics Association Special Volume*, **51**, 167-186.
- Brand, L.E., 1994. Physiological ecology of marine coccolithophores. In Winter, A. and Siesser, W.G. (ed.) *Coccolithophores*. Cambridge University Press, Cambridge, pp. 39-49.
- Brown, C. W. and Yoder, J. A. (1994). Coccolithophorid Blooms in the Global Ocean. *Journal of Geophysical Research-Oceans* **99** (C4), 7467-7482.
- Charlson, R.J., Lovelock, J.E., Andrea, M.O. and Warren, S.G. 1987. Oceanic phytoplankton, atmospheric sulfur, cloud albedo and climate. *Nature*, **326**, 655-661.
- Chisholm, S.W. 1981. Temporal patterns of cell division in unicellular algae. In Platt, T. (ed.) *Physiological Bases of Phytoplankton Ecology*. *Canadian Bulletin of Fisheries and Aquatic Science*, **210**, 150-181.
- Cochran, P.K. and Paul, J.H. 1998. Seasonal abundance of lysogenic bacteria in a subtropical estuary. *Applied and Environmental Microbiology*, **64**, 2308-2312.
- Feely, R.A., Sabine, C.L., Lee, K., Berelson, Will., Kleypas, J., Fabry, V.J. and Millero, F.J. 2004. Impact of Anthropogenic CO₂ on the CaCO₃ System in the Oceans. *Science*, **305**, 362-366.

- Green, J.C., Course, P.A. and Tarran, G.A. 1996. The life cycle of *Emiliana huxleyi*: a brief review and a study of ploidy levels analysed by flow cytometry. *Journal of Marine Systems*, **9**, 33-44.
- Guillard, R.R.L. 1975. Culture of phytoplankton for feeding marine invertebrates. In Smith, W.L. and Chanley, M.H. (eds.) *Culture of Marine Invertebrate Animals*. Plenum Press, New York, USA, pp. 26-60
- Guillard, R.R.L. and Ryther, J.H. 1962. Studies of marine planktonic diatoms. I. *Cyclotella nana* Hustedt and *Detonula confervacea* Cleve. *Canadian Journal of Microbiology*, **8**, 229-239.
- Hill, R.W., White, B.A., Cottrell, M.T. and Dacey, J.W.H. 1998. Virus-mediated total release of dimethylsulfoniopropionate from marine phytoplankton: a potential climate process. *Aquatic Microbial Ecology*, **14**, 1-6.
- Jacquet, S., Heldal, M., Igelesias-Rodriguez, D., Larsen, A., Wilson, W. and Bratbak, G. 2002. Flow cytometric analysis of an *Emiliana huxleyi* bloom terminated by viral infection. *Aquatic Microbial Ecology*, **27**, 111-124.
- Jeffrey, W.H., Kase, J.P. and Wilhelm, S.W. 2000. UV radiation effects on heterotrophic bacterioplankton and viruses in marine ecosystems. In de Mora, S., Demers, S. and Vernet, M. (eds.) *The effects of UV radiation in the marine environment*, *Cambridge Environmental Chemistry Series 10*. Cambridge University Press, Cambridge, pp. 206-236.
- Jordan, R.W. 2001 Haptomonads (online). Encyclopaedia of Life Sciences. Available from <http://www.els.net> [accessed 15 December 2003]
- Klaveness, D. & Paasche, E. 1979. Physiology of coccolithophorids. In *Biochemistry and Physiology of Protozoa*, 2nd edn, vol. 1, ed. M Levandovsky, S.H. Hunter, pp. 191-213. Academic Press, London.

- Laguna, R., Romo, J., Read, B.A. and Wahlund, T.M. 2001. Induction of Phase Variation Events in the Life Cycle of the Marine Coccolithophorid *Emiliana huxleyi*. *Applied and Environmental Microbiology*, **67** (9), 3824-3831.
- Larsen, A., Castberg, T., Sandaa, R.A., Brussaard, C.P.D., Egge, J., Heldal, M., Paulino, A., Thyrraug, R., van Hannen, E.J., and Bratbak, G. 2001. Population dynamics and diversity of phytoplankton, bacteria and viruses in a seawater enclosure. *Marine Ecology Progress Series*, **221**, 47-57.
- Malin, G., Turner, S. M. et al. (1992). Sulfur - the Plankton Climate Connection. *Journal of Phycology* **28** (5), 590-597.
- Malin, G., Turner, S.M., Liss, P.S., Holligan, P.M. and Harbour, D.S. 1993. Dimethylsulphide and dimethylsulphoniopropionate in the northeast Atlantic during the summer coccolithophore bloom. *Deep-Sea Research I*, **40**, 1487-1508.
- Matrai, P.A. and Keller, M.D. 1993. Dimethylsulphide in a large-scale coccolithophore bloom in the Gulf of Maine. *Continental Shelf Research*, **13**, 831-843.
- McIntyre, A., Bé, A.W.H. and Roche, M.B. 1970. Modern Pacific coccolithophorida: a paleontological thermometer. *Transactions of the New York Academy of Sciences*. **32**, 720-731.
- Murray, A.G. 1995. Phytoplankton exudation: exploitation of the microbial loop as a defence against algal viruses. *Journal of Plankton Research*, **17**, 1079-1094.
- Murray, A.G. and Jackson, G.A. 1992. Viral dynamics: a model of the effects of size, shape, motion and abundance of single-celled planktonic organisms and other particles. *Marine Ecology Progress Series*, **89**, 103-116.
- Nanninga, H.J., and Tyrrell, T. 1996. Importance of light for the formation of algal blooms by *Emiliana huxleyi*. *Marine Ecology Progress Series*, **136**, 195-203.

- Okada, H. and Honjo, S. 1973. The distribution of oceanic coccolithophorids in the Pacific. *Deep Sea Research*, **20**, 355-374.
- Paasche, E., 2002. A review of the coccolithophorid *Emiliana huxleyi* (Prymnesiophyceae), with particular reference to growth, coccolith formation, and calcification-photosynthesis interactions. *Phycologia*, **40**, 503-529.
- Riebesell, U., Zondervan, I., Rost, B., Tortell, P.D., Zeebe, R.E. & Morel, F.M.M., 2000. Reduced calcification of marine plankton in response to increased atmospheric CO₂. *Nature*, **407**, 364-367.
- Riemann, L. & Middelboe, M., 2002. Viral lysis of marine bacterioplankton: implications for organic matter cycling and bacterial clonal composition. *Ophelia*, **56**, 57-68.
- Sabine, C.L., Feely, R.A., Gruber, N., Key, R.M., Lee, K., Bullister, J.L., Wanninkhof, R., Wong, C.S., Wallace, D.W.R., Tilbrook, B., Millero, F.J., Peng, T.H., Kozyr, A., Ono, T. and Rios, A.F. 2004. The Oceanic Sink for Anthropogenic CO₂. *Science*, **305** (5682), 367-371.
- Schroeder, D.C., Oke, J., Malin, G. and Wilson, W.H. 2002. Coccolithovirus (Phycodnaviridae): Characterisation of a new large dsDNA algal virus that infects *Emiliana huxleyi*. *Archives of Virology*, **147** (9), 1685-1698.
- Takahashi, T. 2004. The Fate of Industrial Carbon Dioxide. *Science*, **305**, 352-353.
- Thyrhaug, R., Larsen, A., Brussaard, C.P.D. & Bratbak, G., 2002. Cell cycle dependent virus production in marine phytoplankton. *Journal of Phycology*, **38**, 338-343.
- Turner, S.M., Malin, G., Liss, P.S., Harbour, D.S. and Hollinghan, P.M. 1988. The Seasonal variation of dimethyl sulphide and dimethylsulfoniopropionate concentrations in nearshore waters. *Limnology and Oceanography*, **33** (3), 364-375.

- Tyrrell, T. and Taylor, A.H. 1996. A modelling study of *Emiliana huxleyi* in the NE Atlantic. *Journal of Marine Systems*, **9**, 83-112.
- Van Bleijswijk, J.D.L. 1996. Ecophysiology of the calcifying marine alga *Emiliana huleyi*. Masters Thesis. *Netherlands Institute for Sea Research on Texel*, Rijksuniversiteit Groningen.
- Vaulot, D. and Chisholm, S. W. 1987. A simple model of the growth of phytoplankton populations in light/dark cycles. *Journal of Plankton Research*. **9**, 345-366.
- Wilhelm, S, W. & Suttle, C.A., 1999. Viruses and nutrient cycles in the sea. *Bioscience*, **49**, 781-788.
- Wilson, W.H., Tarran, G. & Zubkov, M.V., 2002a. Virus dynamics in a coccolithophore-dominated bloom in the North Sea. *Deep Sea Research II*, **49**, 2951-2963.
- Wilson, W.H., Tarran, G., Schroeder, D., Cox, M., Oke, J. & Malin, G., 2002b. Isolation of viruses responsible for the demise of an *Emiliana huxleyi* bloom in the English channel. *Journal of the Marine Biological Association of the U.K.* **82**, 369-377.
- Young, J.R., Davis, S.A., Brown, P.R. & Mann, S., 1999. Coccolith Ultrastructure and biomineralistaion. *Journal of Structural Biology*, **126**, 195-215.
- Young, J.R. 1994. Functions of coccoliths. In Winter, A. and Siesser, W.G. (ed.) *Coccolithophores*. Cambridge University Press, Cambridge, pp. 63-82.